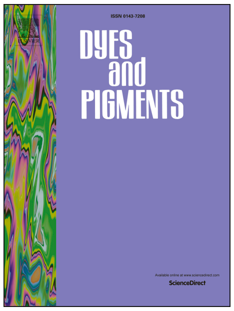

Synthesis and photophysical properties of fluorescent dyes based on triphenylamine, diphenylamine, diphenyl sulfone or triphenyltriazine derivatives containing an acetylene linkage group

Kyung-Won Kim, Su-Hyeon Kwon, Byung-Jun Lee, Sung-Ok Ahn, Ju-Hong Lee, Jae-Hong Choi

PII: S0143-7208(20)31160-8

DOI: https://doi.org/10.1016/j.dyepig.2020.108617

Reference: DYPI 108617

To appear in: *Dyes and Pigments*

Received Date: 1 May 2020

Revised Date: 31 May 2020

Accepted Date: 1 June 2020

Please cite this article as: Kim K-W, Kwon S-H, Lee B-J, Ahn S-O, Lee J-H, Choi J-H, Synthesis and photophysical properties of fluorescent dyes based on triphenylamine, diphenylamine, diphenyl sulfone or triphenyltriazine derivatives containing an acetylene linkage group, *Dyes and Pigments* (2020), doi: https://doi.org/10.1016/j.dyepig.2020.108617.

Synthesis and photophysical properties of fluorescent dyes based on triphenylamine, diphenylamine, diphenyl sulfone or triphenyltriazine derivatives containing an acetylene linkage group

Kyung-Won Kim[a], Su-Hyeon Kwon[b], Byung-Jun Lee[b], Sung-Ok Ahn[b], Ju-Hong Lee[b], Jae-Hong Choi[b,*]

[a] *Advanced Organic Materials Science and Engineering, Kyungpook National University, Daegu 41566, Korea.*

[b] *Department of Textile System Engineering, Kyungpook National University, Daegu 41566, Korea.*

*jaehong@knu.ac.kr

Keywords : acetylene linkage; carbazole; naphthalimide; triphenylamine; fluorescent dye

Abstract

In this study, ten fluorescent dyes were prepared based on three different kinds of central moiety, such as triphenylamine, diphenylsulfone or triphenyltriazine, which was coupled to either carbazole or naphthalimidinyl group via an acetylene linkage group. *N*-*n*-Butyl-carbazole, *N*-phenyl-carbazole or *N*-*n*-butyl-naphthalimide was coupled to the individual central moiety of triphenylamine, diphenyl sulfone, 2,4,6-triphenyl-1,3,5-trazine or diphenylamine using a Sonogashira coupling reaction in the final step. All dyes were confirmed their chemical structure by ^{1}H NMR, GC-Mass and elemental analyses. The absorption properties and thermal stabilities of the fluorescent dyes were examined. Density Functional Theory (DFT) and Time-Dependent DFT calculations were carried out, in addition to geometry simulation, by using the Gaussian 09 program. In terms of fluorescence properties in this series, two dyes based on diphenyl sulfonyl and three dyes based on triphenylamine substituted by 1~3 of *N*-*n*-butyl-carbazole exhibited a blue emission, whereas three dyes based on triphenylamine substituted by 1~3 of *N*-*n*-butyl-naphthalimide were observed by a red emitter which can be attributable to both effects the bathochromic shifts in absorption maxima and larger Stokes shifts. In case of corresponding 2,4,6-triphenyl-1,3,5-trazine central moiety coupled to a carbazole ring, a green fluorescence was emitted. Results revealed that the fluorescence of the dyes is affected by the electron-donating strength of the acetylene linkages involved in the π-conjugation systems of the dyes.

1. Introduction

Some fluorescent dyes based on 1,8-naphthalimide derivatives containing an ethynyl linkage group or an acetylene analogous for blue or red light emission [1-3]. One of interesting uses for these fluorescent dyes can be applied to improve agricultural productivity when dyes supply the efficient blue or red light which is contained in the PE film for a green house. Hence, light conversion films have been developed and have attracted attention. Light conversion films do not use artificial external energy; these films integrate wavelength favorable for photosynthesis with sunlight, and these films increase the efficiency of photosynthesis. Compared to artificial LED lights, the light conversion films are advantageous due to that additional equipment and energy are not required leading to lower cost and improved agricultural productivities [4-11]. Recently, a naphthalimde-coumarin conjugate based dye was reported that contained an acetylene group between naphthalimide and coumarin moieties to provide a blue emission of 433 nm with a quantum yield of 0.78, however the thermal stabilities for this dye was not discussed [12]. As a similar series of 1,8-naphthalimide based dyes connected by an imine linkage group with *N*-ethylcarbazole or some other moieties were also prepared to evaluate their thermal and luminescent properties. Among these dyes, *N*-ethylcarbazole based analogue exhibited a green emission of 501 nm in $CHCl_3$ which was shifted 161 nm from its absorption maximum of 340 nm. In addition the temperature of 5% weight loss by DSC analysis was observed at 363 °C [13]. In case of *N*-phenylcarbazole substituted by a thiophene moiety, a blue fluorescence of 442 nm was observed [14].

Naphthalimide-based fluorescent dyes have been studied as one of the blue emitting chromophores featuring their acceptable durability as well as good light fastness, where comparatively larger Stokes shifts can afford a blue emission from maximum absorption in the range of 300 to 390 nm. As another kind of fluorescent dyes, triphenylamine based ones, which exhibits excellent purity and luminous efficiency as well as excellent thermal stability and photophysical properties, have been also studied. The acetylene linkage was often used by a linkage group of fluorescent dye molecules due to its high quantum yield and comparatively good thermal stabilities [15-23].

However, there have been very limited literatures reporting red fluorescent emissions by naphthalimide or triphenylamine based dyes, it is required to study the possibility to prepare dyes featuring extended emission maximum upto red light ranges.

In this study, ten fluorescent dyes were prepared by varing three different kinds of central moiety, such as triphenylamine, diphenylsulfone or triphenyltriazine, which was coupled to either carbazole or naphthalimidinyl group via an acetylene linkage group, so that the effects of a central moiety and substituted ring system via an acetylene linkage onto the absorption maxima, Stokes shift and resultant quantum yields were investigated.

2. Experimental

2.1. Materials and instrumentation

1,8-Naphthalic anhydride (Sigma Aldrich), carbazole (Sigma Aldrich), triphenylamine (Sigma Aldrich), chlorosulfonic acid (TCI Chemical) and triflic acid (TCI Chemical) were used as the starting materials for synthesizing fluorescent dyes with an acetylene linkage. Based on the dye star synthesis scheme, bromine (Junsei Chemical), KI (Ducksan), KIO_3 (Sigma Aldrich), n-butylamine (TCI Chemical), 1-bromobutane (TCI Chemical), 2-methyl-3-butyn-2-ol (Sigma Aldrich), bromobenzene (TCI Chemical) and 4-Bromobenzonitrile(TCI Chemical) were used. Cuprous iodide (Sigma Aldrich), triphenylphosphine (AlfaAesar), and bis(triphenylphosphine)palladium(□)dichloride (Sigma Aldrich) were used as the catalyst for Sonogashira coupling, and triethylamine (TCI Chemical) was used as the base. Other reagents included chloroform (TCI Cheminal), dimethylformamide (DMF, Sigma Aldrich), acetic acid (Ducksan), tetrahydrofuran (Ducksan), toluene (Ducksan), methanol (Samchun Chemicals), ethanol (Samchun Chemicals), methylene chloride (TCI Chemical), ammonia water (Ducksan), n-hexane (Samchun), ethyl. All of the above reagents are first-grade reagents, which are the directors of acetate (Samchun Chemicals), methylene chloride (Samchun Chemicals), and potassium hydroxide (Ducksan).

High-performance liquid chromatography (HPLC, Acme 9000, Young-Lin, Korea) was employed to analyze the purity of the fluorescent dyes and the intermediates; mass spectra were recorded on a gas chromatography–mass spectrometry (GC–MS; 7890/A-5975C GC/MSD, Agilent, USA) system; ^{1}HNMR spectra (Advance Digit 500, Bruker, Germany) were recorded in DMSO-d_6 or $CDCl_3$; elemental analysis was carried out on a Flash 200 system (Thermo Fisher, Italy); optical analysis was carried out on a tandem mass spectrometer (LC–MS, Agilent, USA); UV–Visible spectrophotometry was carried out by dissolving samples in 5.0×10^{-5}mol/L of methylene chloride(Thermo Scientific, Evolution 300); and fluorescence spectra were recorded on a fluorescence spectrophotometer (Scinco, Fluoro Mate FS-2) with the samples dissolved in 5.0×10^{-5} mol/L of methylene chloride. PMT voltage was measured by the fluorescence intensity at 500, and quantum yields were calculated using anthracene (Φ=0.36) and rhodamine B (Φ = 0.49 in ethanol) as references for blue and red fluorescence, respectively. Thermal stability was measured at 30 °C/min from 30 °C to 500 °C under nitrogen using a Q600 thermal analysis system (TA Instruments, Japan).

2.2. Dye syntheses

2.2.1. Synthesis of Triphenylamine-based dye intermediates **T1-T3** : Iodination

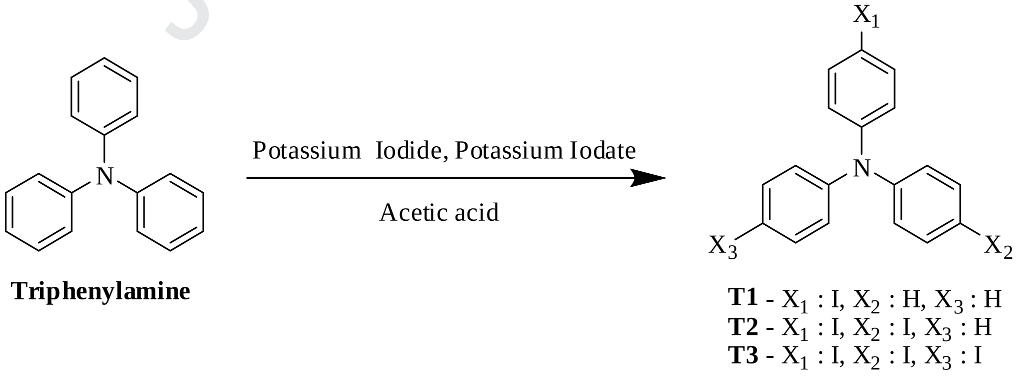

Scheme 1. Synthesis of the triphenylamine derived dye intermediates **T1-T3**.

2.2.1.1. Synthesis of 4-iodo-*N*,*N*-diphenylaniline (**T1**) : Iodination

Potassium iodide (22.2 mmol, 3.68 g) and triphenylamine (33.3 mmol, 8.16 g) were added to acetic acid (100 mL), followed by stirring the mixture at 85 °C for 5 hrs then followed by stirring the mixture for 5 hrs, the temperature was lowered to room temperature. In the next stage, potassium iodate (16.7 mmol, 3.57 g) was slowly added, the temperature was increased to 85 °C, and the reaction was allowed to continue for 5 hrs. When the reaction was completed, the mixture was cooled to room temperature, and water was added. The formed crystals were filtered under reduced pressure, affording crystals. These crystals were recrystallized using methylene chloride, affording the final product in 62.5 % yield. ^{1}H NMR (400MHz, DMSO-d_6): 6.95(d, J = 8.6 Hz, *2H*, ArH), 7.00(d, J = 8.2 Hz, 4H, ArH), 7.08(d, J = 7.8 Hz, 2H, ArH), 7.24(d, J = 8.6 Hz, 4H, ArH), 7.50(d, J = 8.2 Hz, 2H, ArH); HRMS (m/z, MALDI): $[M + H]^+$ calculated for $C_{18}H_{14}IN$: 371.2129; found 371.2132; Elemental analyses, found C, 58.31; H, 3.79; I, 34.14; N, 3.76; '$C_{18}H_{14}IN$' requires C, 58.24; H, 3.77; I, 34.21; N, 3.77.

2.2.1.2. Synthesis of 4-iodo-*N*-(4-iodophenyl)-*N*-phenylaniline (**T2**) : Iodination

Potassium iodate (56 mmol, 12 g), potassium iodide (80 mmol, 13.5 g), and triphenylamine (60 mmol, 15g) were added to acetic acid (340 mL), followed by stirring the mixture at 80 °C for 1hrs. Secondly, after stirring the mixture for 1 hr, water (30 mL) was added, and the mixture was stirred at 80 °C for 6 hrs. The generated crystals were filtered under reduced pressure, affording crystals. Thesecrystals were recrystallized using methyl chloride, affording the final product in 51.9 % yield. ^{1}H NMR (400MHz, DMSO-d_6): 6.95(d, J = 8.6 Hz, 4H, ArH), 7.00(d, J = 8.2 Hz, 2H, ArH), 7.08(d, J = 7.8 Hz, 1H, ArH), 7.24(d, J = 8.6 Hz, 2H, ArH), 7.50(d, J = 8.2 Hz, 4H, ArH); HRMS (m/z, MALDI): $[M + H]^+$ calculated for $C_{18}H_{13}I_2N$: 497.1095; found 497.1038; Elemental analyses, found C, 43.41; H, 2.59; I, 51.04; N, 2.80; '$C_{18}H_{13}I_2N$' requires C, 43.48; H, 2.62; I, 51.09; N, 2.82.

2.2.1.3. Synthesis of tris(4-iodophenyl)amine (**T3**) : Iodination

Potassium iodide (88 mmol, 14.72 g) and triphenylamine (40 mmol, 9.8 g) were added to acetic acid (300 mL), followed by stirring the mixture at 110 °C for 1 hr. Secondly, after stirring the mixture for 1 hr, the temperature was lowered to 80 °C. After slowly adding potassium iodate (44 mmol, 7.3 g), the solution was heated to 110 °C, and the reaction was allowed to continue for 6 hrs. When the reaction was completed, the solution was cooled to room temperature, and water was added. The generated crystals were filtered under reduced pressure, affording crystals. These crystals were recrystallized using methyl chloride, affording the final product in 62.5 % yield. ^{1}H NMR (400MHz, DMSO-d_6): 6.95(d, J = 8.6 Hz, 6H, ArH), 7.50(d, J = 8.2 Hz, 6H, ArH); HRMS (m/z, MALDI): $[M + H]^+$ calculated for $C_{18}H_{12}I_3N$: 623.0061; found 623.0090; Elemental analyses, found C, 34.62; H, 1.89; I, 61.07; N, 2.18; '$C_{18}H_{12}I_3N$' requires C, 34.69; H, 1.93; I, 61.14; N, 2.25.

2.2.2. Synthesis of 4,4'-sulfonylbis(bromobenzene) (**S1**):

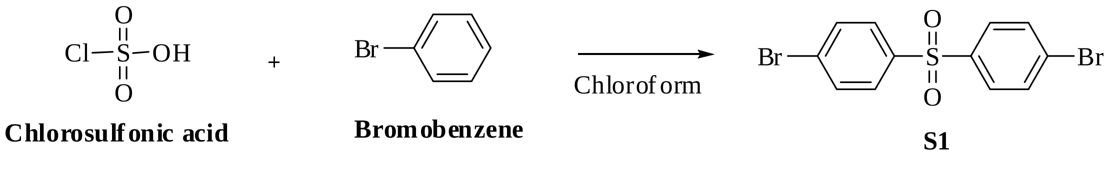

Scheme 2. Synthesis of the diphenyl sulfone derived dye intermediates **S1**.

Chlorosulfonic acid (10 mmol, 1.1 g) was added to Chloroform (25 ml), followed by stirring the mixture with ice-bath at -15°C for 30 min. After slowly adding bromobenzene (20 mmol, 3.1 g), the solution was heated to 50 °C for 2 hr. When the reaction was completed, the solution was cooled to room temperature, and ice water was added. The generated crystals were filtered under reduced pressure, affording crystals. These crystals were recrystallized using methyl chloride, affording the final product in 68.7 % yield. ^{1}H NMR (500MHz, DMSO-d_6) 7.72(d, J = 8.1 Hz, 4H, ArH), 7.77(d, J = 8.1 Hz, 4H, ArH); HRMS (m/z, MALDI): $[M + H]^+$ calculated for $C_{12}H_8Br_2O_2S$: 376.0618; found 376.0636; Elemental analyses, found C, 38.30; H, 2.11; Br, 42.46; O, 8.47; S, 8.49; calculated for $C_{12}H_8Br_2O_2S$ C, 38.33; H, 2.14; Br, 42.49; O, 8.51; S, 8.53.

2.2.3. 2,4,6-Tris(4-bromophenyl)-1,3,5-triazine (**A1**) : Trimerization

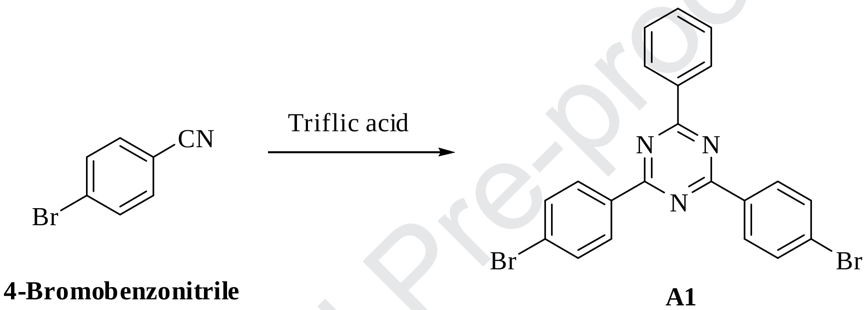

Scheme 3. Synthesis of the triazine derived dye intermediates **A1**.

Trifilic acid (6 mL) was stirred under 0 °C for 30 mins and 4-Bromobenzonitrile (10 mmol, 2 g) was slowly added to the solution. The solution was stirred under 0 °C for 2hrs. After stirring, the solution was stirred under room temperature for 20hrs. Water (50 mL) was added to the solution after stirring was completed, and sodium hydroxide was used to neutralize. After rinsing with methylene chloride (500 mL) and water (500 mL), the obtained organic layer was washed with $MgSO_4$ to remove water, followed by evaporation to obtain the reactant. The obtained reaction product was recrystallized using toluene, affording the final product in 90.9% yield. ^{1}H NMR (500MHz, DMSO-d_6) 7.67(m, 12H, ArH), HRMS (m/z, MALDI): $[M + H]^+$ calculated for $C_{21}H_{12}Br_3N_3$: 546.0504; found 546.0519; Elemental analyses, found C, 46.20; H, 2.20; Br, 43.87; N, 7.68 calculated for $C_{21}H_{12}Br_3N_3$ C, 46.19; H, 2.22; Br, 43.90; N, 7.70.

2.2.4. Synthesis of carbazole-based dye intermediates **C1-C7**

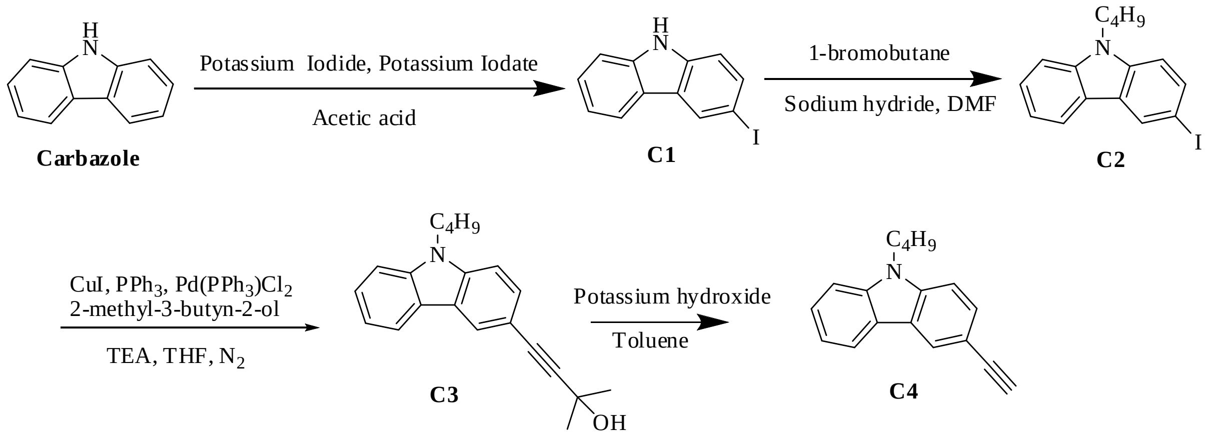

Scheme 4. Synthesis of the carbazole derived dye intermediates **C1**-**C4** [1].

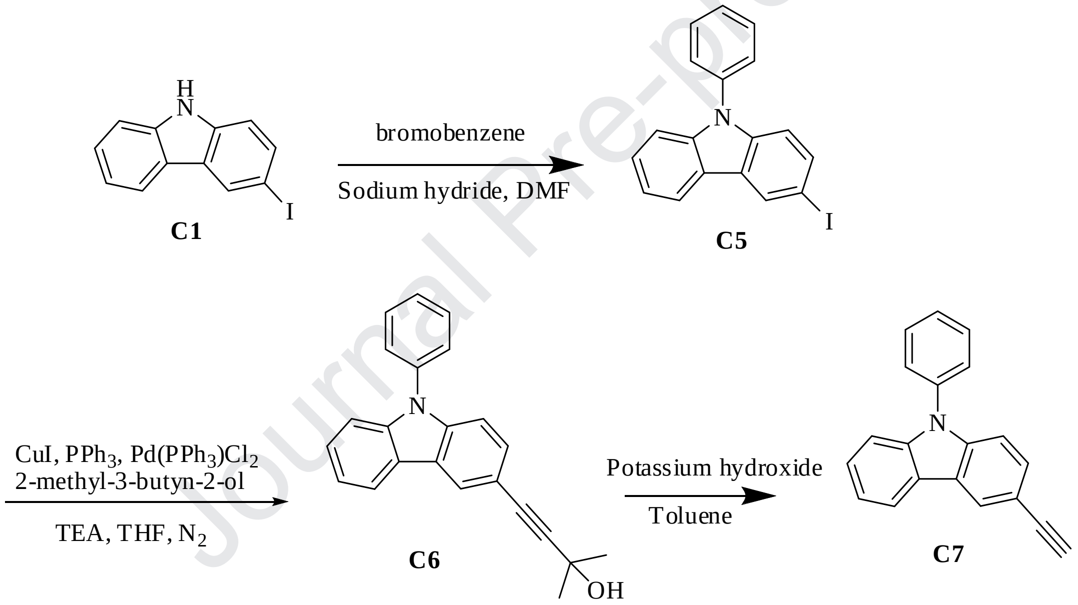

Scheme 5. Synthesis of the carbazole derived dye intermediates **C5**-**C7**.

2.2.4.1. Synthesis of 3-iodo-9*H*-carbazole (**C1**) : Iodination [1]

Potassium iodide (22.2 mmol, 3.68 g) and 9H-carbazole (33.3 mmol, 5.57 g) were added into acetic acid (100 mL), followed by stirring at 110 °C for 1hrs. Second, after stirring the mixture for 1 hr, the temperature was lowered to 80 °C. Finally, potassium iodate (16.7 mmol, 3.57 g) was slowly added, the temperature was increased to 100 °C, and the reaction was allowed to continue for 10 min. When the reaction was completed, the solution was cooled to room temperature, and water was added. The formed crystals were filtered under reduced pressure to obtain crystals. These crystals were recrystallized using methyl chloride, affording the final product in 72.7 % yield. ^{1}H NMR (400MHz, DMSO-d_6): 7.20(d, J = 8.3 Hz, 1H, ArH), 7.35(d, J = 8.0 Hz, 1H, ArH), 7.46(d, J = 8.1 Hz, 1H, ArH), 7.50(d, J = 1.8 Hz, 1H, ArH), 7.63(d, J = 8.1 Hz, 1H, ArH), 7.93(s, 1H, ArH), 8.19(s, 1H, ArH), 11.66(s, 1H, NH); HRMS (*m*/*z*, MALDI): [M + H]$^+$ calculated for $C_{12}H_8IN$: 293.1019; found 293.1051; Elemental analyses, found C, 49.15; H, 2.69; I, 43.23; N, 4.71; ‘$C_{12}H_8IN$’ requires C, 49.17; H, 2.75; I, 43.30; N, 4.78.

2.2.4.2. Synthesis of 9-butyl-3-iodo-9*H*-carbazole (**C2**) : Alkylation [1]

First, 60 % of NaH (4.25 mmol, 0.17 g) and intermediate **C1** (2.9 mmol, 0.85 g) were stirred at 80 °C for 1 h in DMF (5 mL). Second, after the solution was stirred for 1 hr, 1-bromobutane (4.35 mmol, 0.59 g) was added. When the reaction was completed, the solution was poured into warm water. The formed crystals were filtered under reduced pressure to obtain crystals. These crystals were recrystallized using ethanol, affording the final product in 89.7 % yield. ^{1}H NMR (400MHz, DMSO-d_6): 0.89(t, J = 6.5 Hz, 3H, CH_3), 1.26(m, 2H, CH_2), 1.74(m, 2H, CH_2), 4.16(t, J = 7.4 Hz, 2H, CH_2), 7.35(m, 1H, ArH), 7.46(d, J = 8.0 Hz, 2H, ArH), 7.54(m, 1H, ArH), 7.64(s, 1H, ArH), 7.93(s, 1H, ArH), 8.17(s, 1H, ArH); HRMS (*m/z*, MALDI): $[M + H]^+$ calculated for $C_{16}H_{16}IN$: 349.2071; found 349.2066; Elemental analyses, found C, 55.01; H, 4.57; I, 36.24; N, 4.07; ‘$C_{16}H_{16}IN$’ requires C, 55.03; H, 4.62; I, 36.34; N, 4.01.

2.2.4.3. Synthesis of 4-(9-butyl-9*H*-carbazol-3-yl)-2-methylbut-3-yn-2-ol (**C3**) : Sonogashira coupling [1]

Anhydrous tetrahydrofuran (10 mL) was added to a solution of intermediate **C2** (1 mmol, 349 mg), cuprous iodide (0.05 mmol, 15.9 mg), triphenylphosphine (0.05 mmol, 13.1 mg), and bis(triphenylphosphine) palladium(II) dichloride (0.1 mmol, 115 mg), and the solution was stirred under nitrogen for 15 min. Secondly, after the addition of trimethylamine (10 mL) and stirring for 15 min, 2-methyl-3-butyn-2ol (3 mmol, 252 mg) was added, and the solution was stirred for 30 min, followed by reflux for 1hrs. The solution was cooled after the reaction was completed. Next, the solution was added into ammonia water, and ethyl acetate was used to separate the layers, followed by rinsing with water. The obtained organic layer was washed with $MgSO_4$ to remove water, followed by evaporation to obtain the reactant. The obtained reaction product was purified by column chromatography (absorbent: silica gel, eluent: ethyl acetate/n-hexane), affording the final product in 65.1 % yield. ^{1}H NMR (400MHz, DMSO-d_6): 0.89(t, J = 6.5 Hz, 3H, CH_3), 1.26(m, 2H, CH_2), 1.46(s, 6H, 2xCH_3), 1.74(m, 2H, CH_2), 4.16(t, J = 7.4 Hz, 2H, CH_2), 5.40(s, 1H, OH), 7.24(d, J = 8.0 Hz, 1H, ArH), 7.42(d, J = 8.2 Hz, 2H, ArH), 7.55(m, 2H, ArH), 7.71(s, 1H, ArH), 8.17(d, J = 1.9 Hz, 1H, ArH); HRMS (*m*/*z*, MALDI): $[M + H]^+$ calculated for $C_{21}H_{23}NO$: 305.4098; found 305.4056; Elemental analyses, found C, 82.15; H, 7.51; N, 4.47; O, 5.19; ‘$C_{21}H_{23}NO$’ requires C, 82.25; H, 7.59; N, 4.59; O, 5.24.

2.2.4.4. Synthesis of 9-butyl-3-ethynyl-9*H*-carbazole (**C4**) : Hydrolysis [1]

Intermediate *C3* (1 mmol, 305 mg) and KOH (3 mmol, 168 mg) were charged with anhydrous toluene and refluxed under nitrogen for 3 hrs, and after the reaction was completed, the solution was cooled. The reaction product was filtered under reduced pressure to remove KOH and impurities, followed by evaporation. Finally, the obtained reaction product was purified by flash column chromatography (absorbent: silica gel, eluent: ethyl acetate/n-hexane), affording the final product in 76.4 % yield. ^{1}H NMR (400MHz, $CDCl_3$): 0.89(t, J = 6.5 Hz, 3H, CH_3), 1.26(m, 2H, CH_2), 1.74(m, 2H, CH_2), 3.15(s, 1H, CH), 4.16(t, J = 7.4 Hz, 2H, CH_2), 7.24(d, J = 8.0 Hz, 1H, ArH), 7.33(d, J = 8.2 Hz, 2H, ArH), 7.55(m, 2H, ArH), 7.71(s, 1H, ArH), 8.17(d, J = 1.9 Hz, 1H, ArH); HRMS (*m/z*, MALDI):

[M + H]$^+$ calculated for $C_{18}H_{17}N$: 247.3319; found 247.3353; Elemental analyses, found C, 87.38; H, 6.91; N, 5.56; '$C_{18}H_{17}N$' requires C, 87.41; H, 6.93; N, 5.66.

2.2.4.5. Synthesis of 3-iodo-9-phenyl-9*H*-carbazole (**C5**) : Phenylation

C5 was synthesized using intermediate **C1** (2.9 mmol, 0.85 g) based on the C2 synthetic method using Bromobenzene(12.5mmol, 0.72g) instead of 1-bromobutane, affording the final product in 65.1 % yield. ^{1}H NMR (500MHz, DMSO-d_6) 7.25(t, *J* = 8.4 Hz, 2H, ArH), 7.40(m, 3H, ArH), 7.50(d, *J* = 8.2 Hz, 2H, ArH), 7.58(t, *J* = 8.2 Hz, 2H, ArH), 7.94(d, *J* = 8.2 Hz, 2H, ArH), 8.55(d, *J* = 1.8 Hz, 1H, ArH); HRMS (*m*/*z*, MALDI): [M + H]$^+$ calculated for $C_{18}H_{12}IN$: 369.1973; found 369.1990; Elemental analyses Found C:58.55, H:3.24, I:34.32, N:3.74 calculated for $C_{18}H_{12}IN$ C:58.56, H:3.28, I:34.37 N:3.79.

2.2.4.6. Synthesis of 2-methyl-4-(9-phenyl-9*H*-carbazol-3-yl)but-3-yn-2-ol (**C6**) : Sonogashira coupling

C6 was synthesized using intermediate **C5** (1.5 mmol, 0.5g) based on the **C3** synthetic method, affording the final product in 62.8 % yield. ^{1}H NMR (500MHz, DMSO-d_6) 1.46(s, 6H, CH_3), 5.45(s, 1H, OH), 7.24(m, 3H, ArH), 7.45(m, 3H, ArH), 7.60(d, *J* = 8.1 Hz, 3H, ArH), 7.71(s, 1H, ArH), 7.94(s, 1H, ArH), 8.55(d, *J* = 1.9 Hz, 1H, ArH); HRMS (*m*/*z*, MALDI): [M + H]$^+$ calculated for $C_{23}H_{19}NO$: 325.4000; found 325.4011; Elemental analyses, found C:84.82, H:5.86, N:4.27, O:4.90 calculated for $C_{23}H_{19}NO$ C:84.89, H:5.89, N:4.30, O:4.92.

2.2.4.7. Synthesis of 3-ethynyl-9-phenyl-9*H*-carbazole (**C7**) : Hydrolysis

C7 was synthesized using intermediate **C6** (3 mmol, 1.0g) based on the **C4** synthetic method, affording the final product in 67.1 % yield. ^{1}H NMR (500MHz, DMSO-d_6) 4.05(s, 1H, CH), 7.24(m, 3H, ArH), 7.45(m, 3H, ArH), 7.60(d, *J* = 8.1 Hz, 3H, ArH), 7.71(s, 1H, ArH), 7.94(s, 1H, ArH), 8.55(d, *J* = 1.9 Hz, 1H, ArH); HRMS (*m*/*z*, MALDI): [M + H]$^+$ calculated for $C_{20}H_{13}N$: 267.3221; found 267.3235; Elemental analyses, found C:89.82, H:4.85, N:5.21 calculated for $C_{20}H_{13}N$ C:89.86, H:4.90, N:5.24.

2.2.5. Synthesis of naphthalimidyl dye intermediates **N1**-**N4** [1]

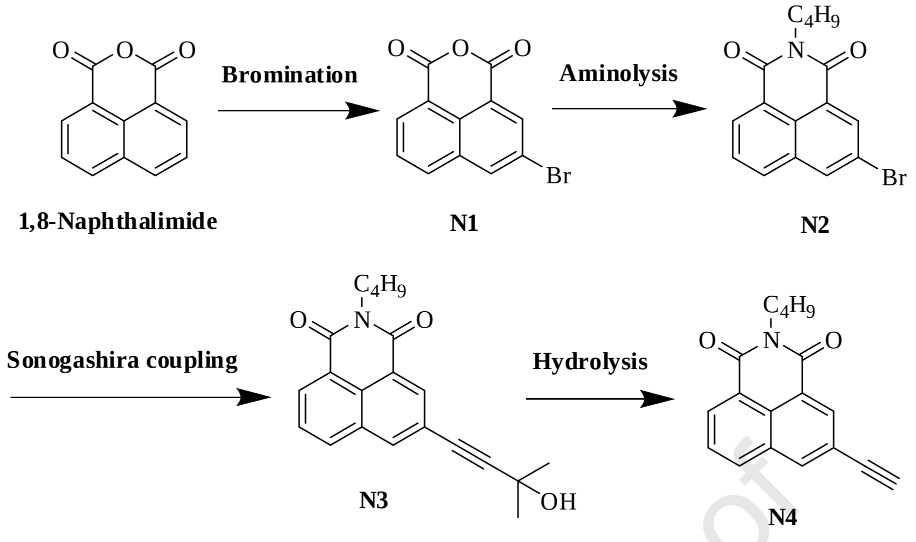

Scheme 6. Synthesis of the naphthalimidyl dye intermediates **N1**-**N4**.

2.2.5.1. Synthesis of 3-Bromo-1,8-naphthalic anhydride (**N1**) : Bromination [1]

Silver(I) sulfate (5 mmol, 1.56 g) and 1,8-naphthalic anhydride (10 mmol, 1.98 g) were added to sulfuric acid (40 mL), and the solution was stirred. Second, after the slow addition of bromine (13 mmol, 6.3 mL), the solution was heated to 60 °C and reacted for 12 hrs. When the reaction was complete, the solution was cooled to room temperature, and water was added. The formed crystals were filtered under reduced pressure to obtain crystals. These crystals were recrystallized using ethanol, affording the final product in 56.7 % yield. ^{1}H NMR (400MHz, DMSO-d_6): 7.39(d, J = 8.2 Hz, 1H, ArH), 7.74(d, J = 7.8 Hz, 1H, ArH), 8.17(s, 1H, ArH), 8.56(d, J = 8.2 Hz, 1H, ArH), 8.58(s, 1H, ArH); HRMS (m/z, MALDI): $[M + H]^+$ calculated for $C_{12}H_5BrO_3$: 277.0684; found 277.0670; Elemental analyses, found C, 52.01; H, 1.79; O, 17.38; '$C_{12}H_5BrO_3$' requires C, 52.02; H, 1.82; O, 17.32.

2.2.5.2. Synthesis of 5-Bromo-2-butyl-1*H*-Benzo [de] isoquinoline-1,3(2*H*)-dione (**N2**) : Aminolysis [1]

Intermediate **N1** (5 mmol, 1.66 g) and n-butylamine (7.5 mmol, 0.74 mL) were added into ethanol (15 mL), and the solution was maintained at reflux conditions for 1 hr. The reaction mixture was cooled after the reaction was completed. Once the solution was completely cooled, the crystals produced were filtered under reduced pressure to obtain crystals. The reaction product was recrystallized using ethanol, affording the final product in 74.2 % yield. ^{1}H NMR (400MHz, DMSO-d_6): 0.90(t, J = 6.5 Hz, 3H, CH_3), 1.30(m, 2H, CH_2), 1.54(m, 2H, CH_2), 3.13(t, J = 7.7 Hz, 2H, CH_2), 7.85(d, J = 7.8 Hz, 1H, ArH), 8.11(d, J = 8.2 Hz, 1H, ArH), 8.40(s, 1H, ArH), 8.50(d, J = 1.9 Hz, 2H, ArH); HRMS (m/z, MALDI): $[M + H]^+$ calculated for $C_{16}H_{14}BrNO_2$: 332.1891; found 332.1899; Elemental analyses, found C, 57.81; H, 4.21; N, 4.15; O, 9.59; '$C_{16}H_{14}BrNO_2$' requires C, 57.85; H, 4.25; N, 4.22; O, 9.63.

2.2.5.3. Synthesis of Butyl-5-(3-hydroxy-3-methylbut-1-ynyl)1*H*-benzo [de] isoquinoline-1,3(2*H*)-dione (**N3**): Sonogashira coupling [1]

Anhydrous tetrahydrofuran (10 mL) was added to a solution of intermediate **N2** (1 mmol, 349 mg), cuprous iodide (0.05 mmol, 15.9 mg), triphenylphosphine (0.05 mmol, 13.1 mg), and bis(triphenylphosphine) palladium(II) dichloride, and the solution was stirred under nitrogen for 15 min. In the next step, after the addition of triethylamine (10 mL) and stirring for 15 min, 2-methyl-3-butyn-2ol (3 mmol, 252 mg) was added, and the solution was stirred for 30 min, followed by reflux for 1 hr. After the reaction was completed, it was cooled. Next, the solution was added into ammonia water, and ethyl acetate was added to separate the layers, followed by rinsing with water. The obtained organic layer was washed with $MgSO_4$ to remove water and then evaporated to obtain a reactant. The obtained reaction product was purified by column chromatography (absorbent: silica gel, eluent: ethyl acetate/n-hexane), affording the final product in 75.8 % yield. ^{1}H NMR (400MHz, DMSO-d_6): 0.90(t, J =6.5 Hz, 3H, CH_3), 1.30(m, 2H, CH_2), 1.46(s, 6H, 2xCH_3), 1.54(m, 2H, CH_2), 3.13(t, *J* = 7.7 Hz, 2H, CH_2), 5.40(s, 1H, OH), 7.90(d, *J* = 8.0 Hz, 1H, ArH), 8.11(d, *J* = 8.2 Hz, 1H, ArH), 8.28(d, *J* = 8.0 Hz, 1H, ArH), 8.45(d, *J* = 1.8 Hz, 2H, ArH); HRMS (*m*/*z*, MALDI): $[M + H]^+$ calculated for $C_{21}H_{21}NO_3$: 335.3922; found 335.3920; Elemental analyses, found C, 75.15; H, 6.34; N, 4.17; O, 14.29; '$C_{21}H_{21}NO_3$' requires C, 75.22; H, 6.27; N, 4.18; O, 14.33.

2.2.5.4. Synthesis of 2-Butyl-5-ethynyl-1*H*-benzo [de] isoquinoline-1,3(2*H*)-dione (**N4**) : Hydrolysis [1]

Intermediate **N3** (1 mmol, 305 mg) and KOH (3 mmol, 168 mg) were charged to anhydrous toluene and refluxed under nitrogen for 3 hrs. Second, after the reaction was completed, the solution was cooled. Next, the reaction product was filtered under reduced pressure to remove KOH and impurities, followed by evaporation. The obtained reaction product was purified by flash column chromatography (absorbent: silica gel, eluent: ethyl acetate/n-hexane), affording the final product in 76.4 % yield. ^{1}H NMR (400MHz, $CDCl_3$): 0.90(t, *J* = 6.5 Hz, 3H, CH_3), 1.30(m, 2H, CH_2), 1.54(m, 2H, CH_2), 3.13(t, *J* = 7.7 Hz, 2H, CH_2), 4.08(s, 1H, CH), 7.90(d, *J* = 8.0 Hz, 1H, ArH), 8.11(d, *J* = 8.2 Hz, 1H, ArH), 8.28(s, 1H, ArH), 8.45(d, *J* = 1.8 Hz, 2H, ArH); HRMS (*m*/*z*, MALDI): $[M + H]^+$ calculated for $C_{18}H_{15}NO_2$: 277.3143; found 277.3141; Elemental analyses, found C, 77.68; H, 5.51; N, 4.96; O, 11.79; '$C_{18}H_{15}NO_2$' requires C, 77.98; H, 5.42; N, 5.05; O, 11.55.

2.2.6. Synthesis of fluorescent dyes **1-6**

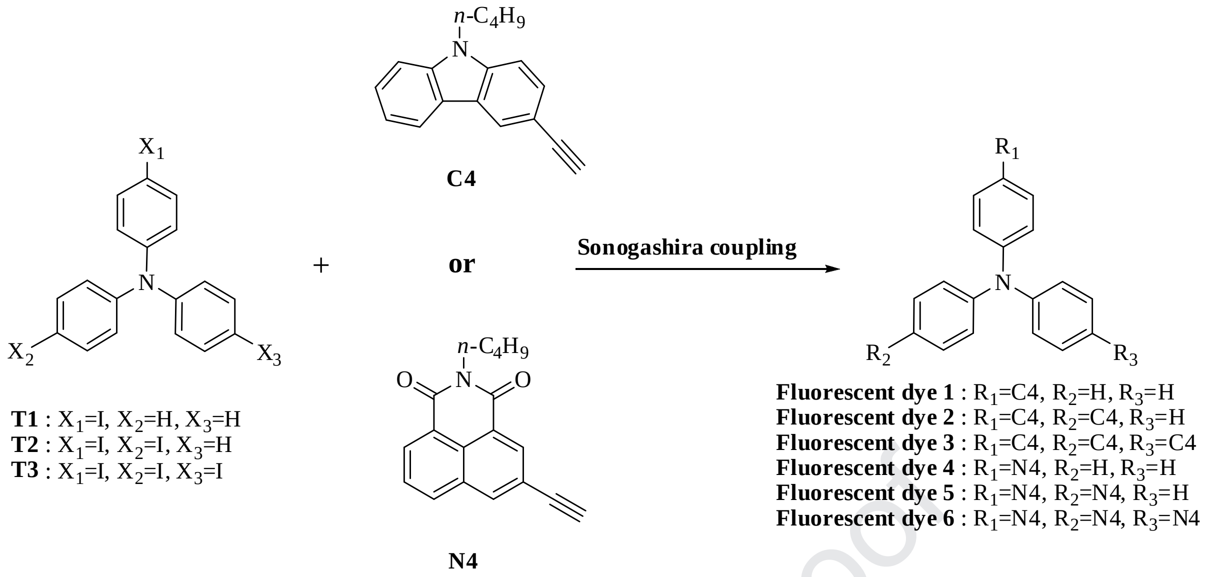

T1 : X_1=I, X_2=H, X_3=H
T2 : X_1=I, X_2=I, X_3=H
T3 : X_1=I, X_2=I, X_3=I

Fluorescent dye 1 : R_1=C4, R_2=H, R_3=H
Fluorescent dye 2 : R_1=C4, R_2=C4, R_3=H
Fluorescent dye 3 : R_1=C4, R_2=C4, R_3=C4
Fluorescent dye 4 : R_1=N4, R_2=H, R_3=H
Fluorescent dye 5 : R_1=N4, R_2=N4, R_3=H
Fluorescent dye 6 : R_1=N4, R_2=N4, R_3=N4

Scheme 7. Synthetic routes of fluorescent dyes **1–6**.

2.2.6.1. Synthesis of fluorescent dye **1** : Sonogashira coupling

First, anhydrous tetrahydrofuran (10 mL) was added to a solution of intermediate **C4** (1 mmol, 349 mg), cuprous iodide (0.05 mmol, 15.9 mg), triphenylphosphine (0.05 mmol, 13.1 mg), and bis(triphenylphosphine) palladium(II) dichloride, and the solution was stirred under nitrogen for 15 min. Secondly, triethylamine (10 mL) was added, and the solution was stirred for 15 min, followed by the addition of intermediate **T1** (1.1 mmol, 305 mg) and stirring for 30 min. Finally, the solution was refluxed for 1 hr. After the reaction was completed, the solution was cooled. Next, the solution was added into ammonia water, and ethyl acetate was used to separate the layers, followed by rinsing with water. The obtained organic layer was washed with $MgSO_4$ to remove water and then evaporated to obtain a reactant. The obtained reaction product was purified by column chromatography (absorbent: silica gel, eluent: ethyl acetate/n-hexane), affording the final product in 73.5 % yield. ^{1}H NMR (400MHz, DMSO-d_6): 0.89(t, J = 6.5 Hz, 3H, CH_3), 1.26(m, 2H, CH_2), 1.74(m, 2H, CH_2), 4.16(t, J = 7.5 Hz, 2H, CH_2), 7.08(m, 6H, ArH), 7.14(m, 2H, ArH), 7.24(m, 9H, ArH), 7.64(m, 3H, ArH), 8.17(d, J = 8.2 Hz, 1H, ArH); ^{13}C NMR (75 MHz, DMSO-d_6, δ, ppm) 147.72, 146.12, 140.65, 140.30, 132.98, 132.95, 129.25, 127.69, 126.44, 124.72, 124.44, 123.39, 122.93, 122.64, 120.74, 120.45, 119.42, 109.37, 108.98, 107.87, 90.45, 86.65, 43.31, 20.07, 13.85; HRMS (m/z, MALDI): $[M + H]^+$ calculated for $C_{36}H_{30}N_2$: 490.6326; found 490.6318; Elemental analyses, found C, 88.11; H, 6.12; N, 5.68; '$C_{36}H_{30}N_2$' requires C, 88.13; H, 6.16; N, 5.71.

2.2.6.2. Synthesis of fluorescent dye **2** : Sonogashira coupling

Fluorescent dye **2** was synthesized using intermediate **C4** (1 mmol, 330 mg) and intermediate **T2** (2.2 mmol, 610 mg) based on the above method, affording the final product in 68.5 % yield. ^{1}H NMR (400 MHz, DMSO-d_6): 0.89(t, J = 6.5 Hz, 6H, 2xCH_3), 1.26(m, 4H, 2xCH_2), 1.74(m, 4H, 2xCH_2), 4.16(t, J = 7.5 Hz, 4H, 2xCH_2), 7.08(d, J = 7.8 Hz, 6H, ArH), 7.14(m, 1H, ArH), 7.51(m, 16H, ArH), 7.75(m, 3H, ArH), 8.17(d, J = 8.2 Hz, 1H, ArH); ^{13}C NMR (75 MHz, DMSO-d_6, δ, ppm) 147.72, 146.12, 140.65, 140.30, 132.98, 132.95, 129.25, 127.69, 126.44, 124.72, 124.44, 123.39, 122.93, 122.64, 120.74, 120.45, 119.42, 109.37, 108.98, 107.87, 90.45, 86.65, 43.31, 31.01, 20.07, 13.85; HRMS (m/z, MALDI): $[M + H]^+$ calculated for $C_{54}H_{45}N_3$: 735.9489; found 735.9483; Elemental analyses, found C, 88.13; H, 6.13; N, 5.69; '$C_{54}H_{45}N_3$' requires C, 88.16; H, 6.12; N, 5.71.

2.2.6.3. Synthesis of fluorescent dye **3** : Sonogashira coupling

Fluorescent dye **3** was synthesized using intermediate **C4** (1 mmol, 330 mg) and intermediate **T3** (3.3 mmol, 915 mg) based on the above method, affording the final product in 53.1 % yield. ^{1}H NMR (400 MHz, DMSO-d_6): 0.89(t, J = 6.5 Hz, 9H, 3xCH_3), 1.26(m, 6H, 3xCH_2), 1.74(m, 6H, 3xCH_2), 4.16(t, J = 7.5 Hz, 6H, 3xCH_2), 7.14(d, J = 8.3 Hz, 6H, ArH), 7.51(m, 19H, ArH), 7.75(m, 5H, ArH), 8.17(d, J = 8.2 Hz, 3H, ArH); ^{13}C NMR (75 MHz, DMSO-d_6, δ, ppm) 146.12, 140.65, 140.30, 132.98, 132.95, 127.69, 123.39, 122.93, 122.64, 120.74, 120.45, 119.42, 109.37, 108.98, 107.87, 90.45, 86.65, 43.31, 31.01, 20.07, 13.85; HRMS (m/z, MALDI): $[M + H]^+$ calculated for $C_{72}H_{60}N_4$: 981.2652; found 981.2665; Elemental analyses, found C, 88.07; H, 6.14; N, 5.65; '$C_{72}H_{60}N_4$' requires C, 88.07; H, 6.12; N, 5.71.

2.2.6.4. Synthesis of fluorescent dye **4** : Sonogashira coupling

Anhydrous tetrahydrofuran (10 mL) was added to a solution of intermediate **N4** (1 mmol, 349 mg), cuprous iodide (0.05 mmol, 15.9 mg), triphenylphosphine (0.05 mmol, 13.1 mg), and bis(triphenylphosphine) palladium(II) dichloride, and the solution was stirred under nitrogen for 15 min. Second, after triethylamine (10 mL) was added, and the solution was stirred for 15 min, intermediate **T1** (1.1 mmol, 305 mg) was added, and the solution was stirred for 30 min, followed by reflux for 1hr. After the reaction was completed, the solution was cooled. Next, the cooled solution was added into ammonia water, and ethyl acetate was used to separate the layers, followed by rinsing with water. The obtained organic layer was washed with $MgSO_4$ to remove water, followed by evaporation to obtain a reactant. The obtained reaction product was purified by column chromatography (absorbent: silica gel, eluent: ethyl acetate/n-hexane, affording the final product in 63.7 % yield. ^{1}H NMR (400 MHz, DMSO-d_6): 0.90(t, J = 6.6 Hz, 3H, CH_3), 1.30(m, 2H, CH_2), 1.54(m, 2H, CH_2), 3.13(t, J = 11 Hz, 2H, CH_2), 7.08(d, J = 8.3 Hz, 6H, ArH), 7.14(d, J = 8.0 Hz, 2H, ArH), 7.51(d, J = 7.3 Hz, 6H, ArH), 7.89 (d, J = 7.5 Hz, *1H*, ArH), 8.11(d, J = 8.3 Hz, 1H, ArH), 8.28(s, 1H, ArH), 8.42(d, J = 2.0 Hz, 2H, ArH); ^{13}C NMR (75 MHz, DMSO-d_6, δ, ppm) 147.72, 146.12, 138.85, 133.95, 132.95, 130.38, 129.25, 128.37, 125.50, 124.72, 124.44, 124.22, 122.93, 121.56, 107.87, 91.05, 90.45, 55.19, 53.68, 29.73, 20.07, 13.85; HRMS (m/z, MALDI): $[M + H]^+$ calculated for $C_{36}H_{28}N_2O_2$: 520.6150; found 520.6153; Elemental analyses, found C, 83.01; H, 5.42; N, 5.49; O, 6.12; '$C_{36}H_{28}N_2O_2$' requires C, 83.05; H, 5.52; N, 5.42; O, 6.15.

2.2.6.5. Synthesis of fluorescent dye **5** : Sonogashira coupling

Fluorescent dye **5** was synthesized using intermediate **N4** (1 mmol, 330 mg) and intermediate **T2** (2.2 mmol, 610 mg) based on the above method, affording the final product in 65.7 % yield. ^{1}H NMR (400 MHz, DMSO-d_6): 0.90(t, J = 6.6 Hz, 6H, 2xCH_3), 1.30(m, 4H, 2xCH_2), 1.54(m, 4H, 2xCH_2), 3.13(t, J = 11 Hz, 4H, 2xCH_2), 7.08(d, J = 8.3 Hz, 6H, ArH), 7.14(d, J = 8.0 Hz, 1H, ArH), 7.51(d, J = 7.3 Hz, 6H, ArH), 7.90(d, J = 7.5 Hz, 2H, ArH), 8.11(d, J = 8.3

Hz, 2H, ArH), 8.28(s, 4H, ArH), 8.45(d, J = 2.0 Hz, 2H, ArH); ^{13}C NMR (75 MHz, DMSO-d_6, δ, ppm) 147.72, 146.12, 138.85, 133.95, 132.95, 130.38, 129.25, 128.37, 127.69, 125.50, 124.72, 124.44, 124.22, 122.93, 121.56, 107.87, 91.05, 90.45, 55.19, 53.68, 29.73, 20.07, 13.85; HRMS (m/z, MALDI): $[M + H]^+$ calculated for $C_{54}H_{41}N_3O_4$: 795.9137; found 795.9134; Elemental analyses, found C, 81.46; H, 5.14; N, 5.12; O, 8.02; '$C_{54}H_{41}N_3O_4$' requires C, 81.49; H, 5.19; N, 5.28; O, 8.04.

2.2.6.6. Synthesis of fluorescent dye **6** : Sonogashira coupling

Fluorescent dye **6** was synthesized using intermediate **N4** (1 mmol, 330 mg) and intermediate **T3** (2.2 mmol, 610 mg) based on the above method, affording the final product in 51.2 % yield. ^{1}H NMR (400 MHz, DMSO-d_6): 0.90(t, J = 6.6 Hz, 9H, 3xCH_3), 1.30(m, 6H, 3xCH_2), 1.54(m, 6H, 3xCH_2), 3.13(t, J = 11 Hz, 6H, 3xCH_2), 7.08(d, J = 8.3 Hz, 6H, ArH), 7.51(d, J = 8.0 Hz, 6H, ArH), 7.90(d, J = 7.5 Hz, 3H, ArH), 8.11(d, J = 8.3 Hz, 3H, ArH), 8.28(s, 6H, ArH), 8.45(d, J = 2.0 Hz, 3H, ArH); ^{13}C NMR (75 MHz, DMSO-d_6, δ, ppm) 146.12, 138.85, 133.95, 132.95, 130.38, 128.37, 127.69, 125.5, 124.22, 122.93, 121.56, 107.87, 91.05, 90.45, 55.19, 53.68, 29.73, 20.07, 13.85; HRMS (m/z, MALDI): $[M + H]^+$ calculated for $C_{72}H_{54}N_4O_6$: 1071.2124; found 1071.2168; Elemental analyses, found C, 80.28; H, 5.02; N, 5.17; O, 8.26; '$C_{72}H_{54}N_4O_6$' requires C, 80.37; H, 5.08; N, 5.23; O, 8.29.

2.2.7. Synthesis of fluorescent dyes **7-8**

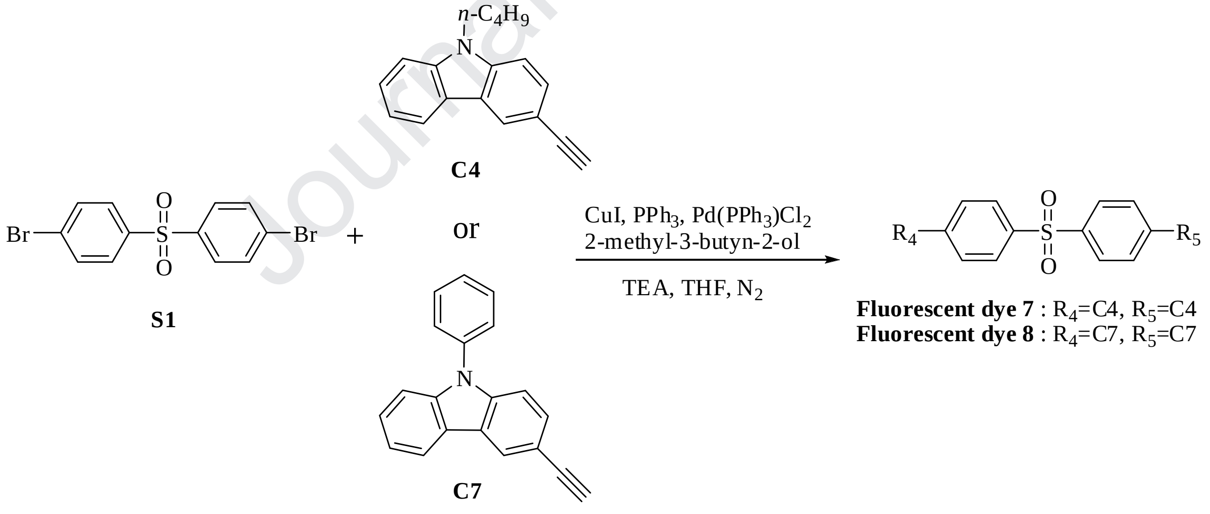

Scheme 8. Synthetic routes of fluorescent dyes **7–8**.

2.2.7.1. Synthesis of blue fluorescent dye **7**

Fluorescent dye **7** was synthesized using intermediate **C4** (16mmol, 3.9g) and intermediate **S1** (8mmol, 3.0g) based on the above method, affording the final product in 75.8 % yield. ^{1}H NMR (500MHz, DMSO-d_6) 0.9(t, J = 6.5 Hz, 6H, CH_3), 1.31(m, 4H, CH_2), 1.74(m, 4H, CH_2),4.16(t, J = 6.4 Hz, 4H, CH_2), 7.32(m, 4H, ArH), 7.47(t, J = 6.6 Hz, 2H, ArH), 7.54(t, J = 8.4 Hz, 2H, ArH), 7.65(t, J = 8.5 Hz, 2H ,ArH), 7.76(d, J = 7.3 Hz, 11H, ArH), 8.36(d, J = 8.4 Hz, 1H, ArH); ^{13}C NMR (75 MHz, DMSO-d_6, δ, ppm) 143.89, 140.70, 140.65, 140.30, 132.98, 132.97, 131.10, 131.04, 129.23, 128.35, 127.69, 126.73, 126.44, 124.65, 123.396, 122.64, 121.00, 120.74, 120.45, 119.42, 117.29, 109.37, 108.98, 90.45, 86.65, 58.06, 49.56, 43.31, 34.74, 31.01, 30.12, 20.07, 13.85; HRMS (*m*/*z*, MALDI): [M + H]$^+$ calculated for $C_{48}H_{40}N_2O_2S$: 708.9020; found 708.9036; Elemental analyses, found C, 81.29; H, 5.65; N, 3.94; O, 4.49; S, 4.49 calculated for $C_{48}H_{40}N_2O_2S$ C, 81.32; H, 5.69; N, 3.95; O, 4.51; S, 4.52.

2.2.7.2. Synthesis of blue fluorescent dye **8**

Fluorescent dye **8** was synthesized using intermediate **C7** (16mmol, 4.2g) and intermediate **S1** (8mmol, 3.0g) based on the above method, affording the final product in 68.3 % yield. ^{1}H NMR (500MHz, DMSO-d_6) 7.72(m, 5H, ArH), 7.45(t, J = 7.9 Hz, 2H, ArH), 7.63(m, 11H, ArH), 7.75(s, 2H, ArH), 7.79(d, J = 7.9 Hz, 8H, ArH), 7.94(d, J = 7.5 Hz, 2H, ArH),, 8.55(d, J = 6.2 Hz, 2H, ArH); ^{13}C NMR (75 MHz, DMSO-d_6, δ, ppm) 141.38, 140.70, 140.62, 137.60, 132.98, 132.97, 129.25, 128.35, 127.69, 127.10, 126.44, 124.72, 123.39, 123.23, 121.00, 120.74, 120.45, 119.42, 109.95, 109.37, 90.45, 86.65; HRMS (*m*/*z*, MALDI): [M + H]$^+$ calculated for $C_{52}H_{32}N_2O_2S$: 748.8824; found 748.8801; Elemental analyses, found C, 83.36; H, 4.27; N, 3.73; O, 4.24; S, 4.25 calculated for $C_{52}H_{32}N_2O_2S$ C, 83.40; H, 4.31; N, 3.74; O, 4.27; S, 4.28.

2.2.8. Synthesis of Fluorescent dyes **9-10**

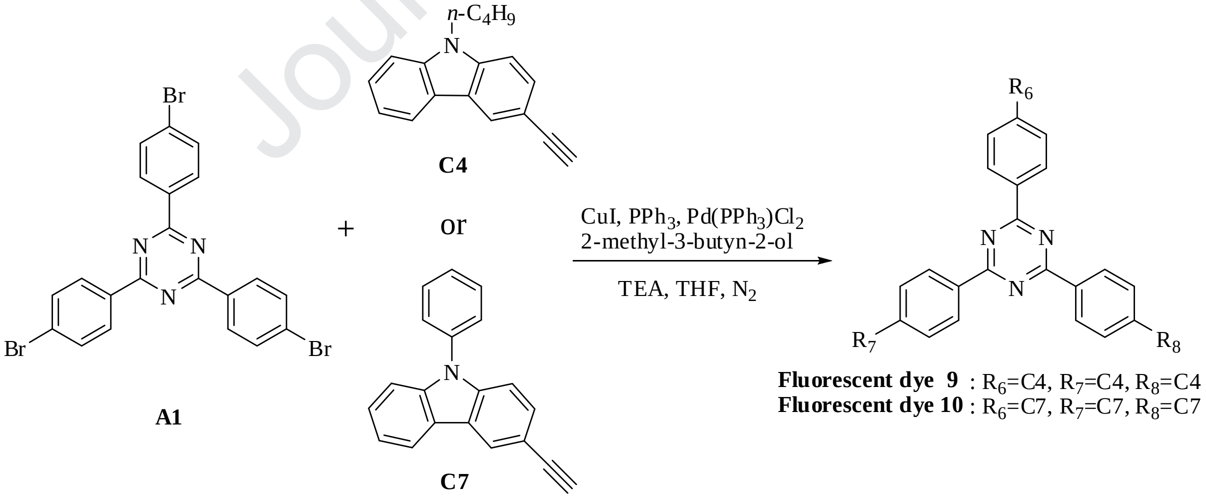

Scheme 9. Synthetic routes of fluorescent dyes **9–10.**

2.2.8.1. Synthesis of green fluorescent dye **9**

A1 (1 mmol, 1.4 g) was added to a solution of triethylamine (30 mL) and toluene (30 mL), and the solution was stirred under nitrogen for 30 min. Secondly, after the addition of copper iodide (0.04 mmol, 0.02 g), triphenylphosphine (0.02 mmol, 0.014 g) and bis(triphenylphosphine) palladium(II) dichloride (0.08 mmol, 0.15 g), and the solution was stirred under nitrogen at 50 °C for 1hrs. After the stirring was completed, intermediate **C4** (3.6 mmol, 2.3 g) was slowly added and followed by reflux for 10 hrs. The solution was filtered under reduced pressure after the reaction was completed. Next, the solution was added into ammonia water and ethyl acetate was used to separate the layers, followed by rinsing with water. The obtained organic layer was washed with $MgSO_4$ to remove water, followed by evaporation to obtain the reactant. Finally, the obtained reaction product was purified by flash column chromatography, affording the final product in 57.3 % yield. ^1H NMR (500MHz, DMSO-d_6) 0.9(t, J = 6.5 Hz, 9H, CH_3), 1.31(m, 6H, 3xCH_2), 1.74(m, 6H, 3x CH_2), 4.16 (m, 6H, 3x CH_2), 7.28(d, J = 7.6 Hz, 3H, ArH), 7.41(t, J = 6.2 Hz, 6H, ArH), 7.62(m, 12H, ArH), 7.75(d, J = 7.6 Hz, 9H, ArH), 8.17(d, J = 5.9 Hz, 3H, ArH); ^{13}C NMR (75 MHz, DMSO-d_6, δ, ppm) 171.46, 143.89, 140.65, 140.30, 131.63, 136.12, 133.00, 132.98, 131.63, 129.23, 129.00, 128.45, 127.69, 126.73, 126.44, 126.02, 124.31, 124.50, 123.39, 122.64, 122.28, 121.58, 120.74, 120.45, 119.42, 116.80, 112.32, 109.37, 108.98, 95.12, 90.45, 86.65, 86.49, 58.06, 49.56, 43.31, 34.74, 31.01, 30.12, 20.07, 13.85; HRMS (m/z, MALDI): $[M + H]^+$ calculated for $C_{75}H_{60}N_6$: 1045.3107; found 1045.3124; Elemental analyses, found C, 86.15; H, 5.77; N, 8.05 calculated for $C_{75}H_{60}N_6$ C, 86.17; H, 5.79; N, 8.04.

2.2.8.2. Synthesis of green fluorescent dye **10**

Fluorescent dye **10** was synthesized using intermediate **C7** (3.6mmol, 2.48g) and intermediate **A1** (1mmol, 1.4g) based on the above method, affording the final product in 61.3 % yield. ^1H NMR (400MHZ, DMSO-d_6) 7.29(m, 9H, ArH), 7.47(m, 9H, ArH), 7.58(m, 9H, ArH), 7.65(d, J = 7.7 Hz, 6H, ArH), 7.75(d, J = 6.9 Hz, 9H, ArH), 7.94(d, J = 5.1 Hz, 3H, ArH), 8.55(d, J = 1.8 Hz, 3H, ArH); ^{13}C NMR (75 MHz, DMSO-d_6, δ, ppm) 171.46, 141.38, 140.62, 137.60, 136.12, 132.98, 131.63, 129.25, 128.45, 127.69, 127.10, 126.44, 124.72, 124.50, 123.39, 123.23, 120.74, 120.45, 119.42, 109.95, 109.37, 90.45, 86.65; HRMS (m/z, MALDI): $[M + H]^+$ calculated for $C_{81}H_{48}N_6$: 1105.2813; found 1105.2823; Elemental analyses, found C, 88.04; H, 4.35; N, 7.57 calculated for $C_{81}H_{48}N_6$ C, 88.02; H, 4.38; N, 7.60.

2.3. Geometry optimization of dyes

Time-dependent density functional theory (TD-DFT) and discrete Fourier transform (DFT) were carried out using the Gaussian 09 programs using the B3LYP, 6-31G as the standard. Hence, the geometry type and Frontier molecular orbital (FMO) are calculated. The core twist angle in intermolecular interactions was analyzed by geometry calculations. In case of naphthalimide, the carbazole angle was calculated from the center of the triphenylamine main body, the angle between the acetylene linkage and naphthalimide, carbazole, and the substituent. The highest occupied molecular orbital (HOMO), lowest unoccupied molecular orbital (LUMO), band gap, and electron density were calculated by FMO calculations.

3. Results and Discussion

3.1 Dye synthesis

Some dyes and intermediates were reported in the previous studies [1,4] featuring their excellent quantum yields for the acetylene-linked fluorescent dyes containing an *n*-butyl or a phenyl ring at the *N*-position of 1,8-naphthalimide. The six fluorescent dyes **1-6** were synthesized in six steps, such as iodination, bromination, alkylation, aminolysis, Sonogashira coupling, and hydrolysis, respectively [1,24].

The iodination of carbazole was carried out under acidic conditions to be substituted at position 3 of carbazole, resulting in reaction yield of 72.7 % yield. In case of extension of the reaction time after the addition of KI the di-iodinated side product formed mainly, thereby the yield of intermediate **C1** was decreased to 42 %.

For *N*-alkylation reaction, the use of polar aprotic solvent, such as DMF, could enhance the reactivity of typical S_N2 reaction. The Sonogashira coupling reaction for 3rd step was successfully carried out by using anhydrous toluene, 10 mol % of bis(triphenylphosphine)palladium(II) dichloride, catalytic amounts of CuI and triphenylphosphine, under these conditions the reaction completed in 1 hr. The reaction rate of the following hydrolysis was increased by the use of comparatively less polar solvent, such as toluene, to compare that of polar solvent, such as *iso*-propylalcohol, resulting in the reaction yield of 76 % [1,25].

In scheme 6, the bromination of 1,8-naphthalic anhydride was carried out under acidic conditions to increase the selectivity to substitute at the 3-position of 1,8-naphthalimide ring, therefore the reaction yield of 56.7 % obtained. The consequent aminolysis reaction was readily carried out using *n*-butylamine and ethanol, under these conditions a reflux for 1 hr provided reaction yield of 74.2 %.

The synthetic schemes for dye intermediates were shown in Scheme 1, Scheme 5, and Scheme 6 for intermediates **T1-3**, intermediate **C4**, and intermediate **N4**, respectively. For the synthetic scheme of six final fluorescent dyes **1-6** was also illustrated in Scheme 7.

Two dyes **7-8** containing a central group of diphenylsulfone were prepared via an intermediate **S1** which was readily synthesized from bromobenzene and chlorosulfonic acid, as shown in Scheme 2, then two bromo atoms were substituted by an acetylene group of *N*-*n*-butyl-carbazole (**C4**) or *N*-phenyl-butyl-carbazole (**C7**) using Sonogashira coupling reaction conditions (Scheme 8) resulting in reasonable reaction yield of 75.8% and 68.3 %, respectively. For a dye intermediate C7, three consequent reaction steps were carried out, as shown in Scheme 6.

The other dyes **9-10** containing a central group of triphenyltriazine were similarly synthesized via an intermediate **A1** which was prepared from 4-bromobenzonitrile and triflic acid, as shown in Scheme 3, then two bromo atoms were also substituted by an acetylene group of *N*-*n*-butyl-carbazole (**C4**) or *N*-phenyl-butyl-carbazole (**C7**) utilising Sonogashira coupling reaction conditions (Scheme 9), where comparatively lower reaction yields were found by 57.3% and 61.3 %, respectively. The higher reaction yields in Sonogashira coupling for dyes **7-8** can be explained by the enhanced electrophilicity of phenyl ring by the presence of an electron-withdrawing group, sulfone group, however a triazine ring also exerted an electron-withdrawing effect therefore the difference in reaction yield was not too significant.

3.2. Absorption and fluorescence spectroscopic properties

Based on the TD-DFT theory using the Gaussian 09 package, the geometry of the six synthesized fluorescent dyes **1-6** was analyzed, and the calculated maximum absorption wavelengths and oscillator strength were summarized in Table 1. By comparison between the calculated absorption maxima and the observed absorption maxima, as shown in Table 2, for dyes **1-6**, it was more reliable to predict for two dyes **1** & **2**, which mono-carbazole or di-carbazole substituted analogous, where the deviations were less than 3 nm [26], whereas the difference of 16 nm became bigger for dye **3** that substituted by tri-carbazole groups. In case of *N*-*n*-butyl-naphthalimidyl analogous, the deviations in absorption maxima were observed by 14 nm, 6 nm, and 9 nm for dyes **4-6**, respectively.

Table 1
Calculated absorption maxima and F values for fluorescent dyes **1–6**.

Fluorescent dyes	Calculated absorption maxima (nm) and F values	
	λ_{max}^{cal}	F
1	330	1.57
2	333	1.39
3	357	1.42
4	418	1.61
5	430	1.57
6	431	1.98

Fluorescent dyes **1**–**3** exhibited the maximum absorbance at 330–341 nm, whereas fluorescent dyes **4–6** bathochromically shifted leading to the absorption maxima at 432–440 nm, as shown in Table 2. It was clearly found that as the number of acetylene group which introduced to the triphenylamine moiety increased, the more bathochromic shift was exhibited for all six dyes **1**-**6**. This red shifts can be attributable to the increased conjugation of π-orbitals, where the presence of three acetylene linkage groups connected to a carbazole ring contributed a bathochromic shift of 11 nm comparing to that of corresponding dye **1** containing an acetylene linkage group. The same red shift was also observed by 8 nm comparing the dye **6** containing three acetylene groups to the corresponding dye **4**. It was unusual that the absorption maxima of dyes **4-6** substituted by naphthalimidyl group were bathochromic shifted significantly comparing to the corresponding dyes **1-3** which containing the same number of carbazole analogous. These red shifts that exhibited in the range of 99 nm ~ 102 nm may be arisen by the more efficient conjugations between central triphenylamine system and naphthalimidyl group via an acetylene linkage group than performed by corresponding carbazole analogous. It can be also assumed that the planarity of π-conjugations throughout the dye molecule for naphthalimidyl based dyes **4**-**6** retained. By comparing the dye **3** containing three *N*-*n*-butylcarbazole substituents to the corresponding dye **9**, the triphenyltriazine ring as a central moiety contributed a bathochromic shift of 21 nm due to the increased π-conjugations by a triazine ring. It was also found that the presence of a *N*-phenyl ring in the carbazole system created a bathochromic shift comparing to that of *N*-*n*-butyl group, therefore dye **10** exhibited a bathochromic shift of 8 nm to the that of dye **9** due to the increased π-conjugations.

Judging from the results of Density Functional Theory (DFT) and Time-Dependent DFT calculations, as in Fig. 2 and Table 3, the carbazole and naphthalimide groups were twisted around the acetylene linkage; therefore the efficiency of π-conjugations decreased led to the increased energy difference between HOMO and LUMO levels. In contrast, the connection between the triphenylamine and the acetylene linkage group retained a planar structure at the center contributing to the delocalization of π orbitals on the dye molecule.

The molar extinction coefficients of fluorescent dyes **1**–**3** ranged from 16,000 to 17,000, which were apparently similar regardless of the difference in the number of carbazole group, and the molar extinction coefficient of fluorescent dyes **4**–**6** ranged from 17,000 to 19,000, where the more substituents the stronger in molar extinction coefficient. It was also found that the dyes **7**-**10** those contained a central group of diphenyl sulfone or 2,4,6-triphenyl-1,3,5-trazine group provided higher molar extinction coefficients to compare that of corresponding dyes **1**-**6**. Although the relationships between the dye structure and the molar extinction coefficients to be often difficult to explain, in these dye series the stronger electron-withdrawing effect by two central moieties can be attributable to the increased molar extinction coefficients. In other words, both the sulfonyl group and triazine ring exerted readily enhanced effects to accept π-electrons from the electron donor, a nitrogen atom in *N*-substituted carbazole ring.

The maximum emission wavelengths of **1**–**3** were observed at 401 nm, 416 nm, and 430 nm, respectively, whereas corresponding dyes **4**–**6** exhibited 580 nm, 595 nm, and 604 nm, respectively, therefore the bigger Stokes' shifts were observed by naphthalimidyl analogous, as summarized in Table 2. As the number of substituent coupled to the central moiety increased, the Stokes shifts tended to increase. It can emphasize that both contributions of the bathochromic shifts at absorption maxima and larger Stokes shifts by naphthalimidyl substituted dyes **4**-**6** readily provide a red emission, whereas the corresponding carbazole substituted dyes emitted a blue fluorescence. In similar, two dyes **9**-**10** containing a central moiety of triphenyltriazine also exhibited comparatively larger Stokes shifts of 140 nm or 145 nm, than that of corresponding triphenylamine based analogous **1**-**3** combined with a bathochromic shift in absorption maxima leading to a green fluorescence emission. As shown in Figure 1, all dye solutions were prepared at 100 ppm concentration in CH_2Cl_2. Strictly speaking, the visual color depths of dye **3** and dye **6** seem to be comparatively stronger than other two dyes among 2 set of blue and red three dyes that coincides to the relative strength of quantum yields, as in Table 2.

In terms of quantum yield, there was a tendency that dyes **7**–**10** containing a central moiety of triphenyltriazine or diphenylsulfone exhibited consistently higher quantum yields of 0.83 to 0.85, whereas the other dyes **1**–**6** varied their quantum yields from 0.34 to 0.89 depending on the substituent. In this series, the highest quantum yield was observed by dye **3** where as the number of substituent, such as *N*-*n*-butyl carbazole or *N*-*n*-butyl naphtalimidyl, increased the higher quantum yield was provided, therefore it can be explained that the enhanced π-conjugations could contribute the stronger emission.

Table 2

Absorption and fluorescence properties of the synthesized dyes.

Fluorescent dyes	λ_{max}^{ab} (nm)	λ_{max}^{em} (nm)	Stokes shift (nm)	ε_{max} ($dm^3\ mol^{-1}\ cm^{-1}$)	Quantum yield
1	330	401	71	16,000	0.68
2	336	416	80	17,000	0.72
3	341	430	89	16,000	0.89
4	432	580	148	17,000	0.34
5	436	595	159	18,000	0.44
6	440	604	164	19,000	0.78
7	346	444	98	43,000	0.83
8	358	452	94	44,000	0.85
9	362	502	140	41,000	0.83
10	370	515	145	42,000	0.85

λ_{max}^{ab}, λ_{max}^{em}: determined in methylene chloride(1.0×10^{-5} mol/L)

Reference: Anthracene.

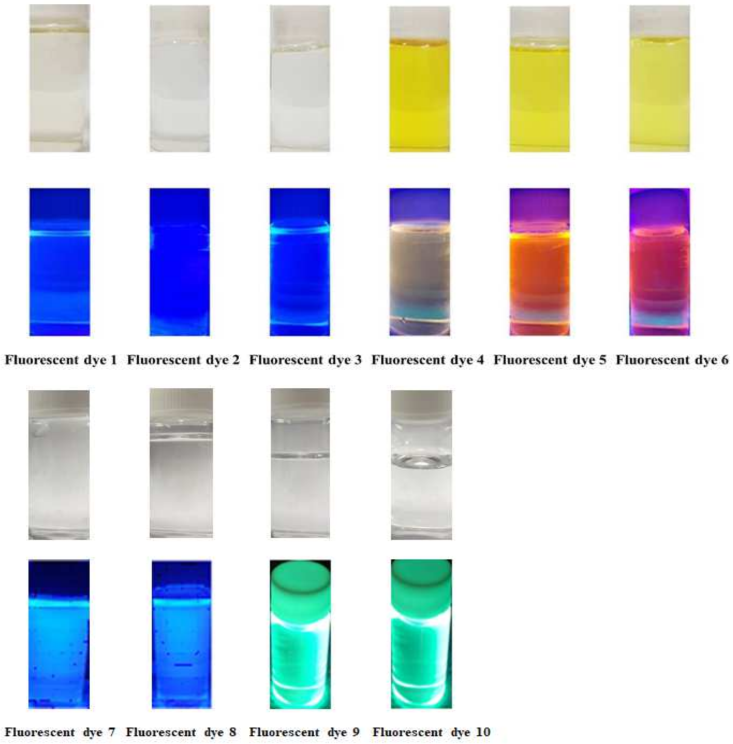

Fig. 1. Optical images of fluorescent dyes **1**–**10** in methylene chloride solutions (100 ppm) under a UV light of 365 nm.

3.3. Calculations of dye structure geometry

The presence of any substituent at the *N*-position of carbazole or naphthalimide ring, it can affect readily the geometry of dyes by the resultant π–π interactions by a substituent. This tendency was observed when the geometry of dye molecule was analyzed on the basis of time-dependent density functional theory (TD-DFT) of the six dyes **1-6** [27-30]. The dihedral angles between central nitrogen atom and three individual phenyl rings were calculated in Table 3, in which *n*-butyl substituent at the *N*-position of the carbazole or naphthalimide ring exhibited a distorted structure with some extents of dihedral angles. The calculated dihedral angles were revealed 0.14 °, 3.13 °, and 3.19 ° for three individual phenyl rings **1**-**3** of dye **1**, where the least distortion was calculated by a carzole substituted phenyl ring **1** due to the efficient conjugation of π-orbitals, thus it can be assumed that dye **1** contained a planar bond, between a carbazole connected acetylene group and phenyl ring **1**, and two comparatively distorted bonds unsubstituted phenyl rings **2**-**3**. In contrast, the dihedral angles of three corresponding bonds for dye **3** were appeared to be 0.48 °, 0.39 °, and 0.42 ° indicating all bonds retained a planar geometry. These calculated results suggested that as the number of substituents to triphenylamine central moiety increased, the planarity of the dyes was comparatively enhanced which mainly related to the efficient π -conjugations between carbazole ring and triphenylamine system.

The similarity of the effect of substituents was also observed by dyes **4-6**, those substituted by corresponding *N*-*n*-butyl-naphthalimide, where the dihedral angles of mono-substituted triphenylamine of dye **4** were calculated as 1.02 °, 3.22 °, 4.02 °, thus phenyl ring **1** retained its planarity but other two analogues **2**-exhibited more distorted angle. The dihedral angles for dye **6** were calculated by 0.97 °, 1.13 °, and 1.31 ° revealing three individual bond angles to be comparatively planar that should be also attributable to the increased conjugations of π-orbitals between naphthalimide, acetylene group and triphenylamine systems. In case of dye **5**, an unsubstituted phenyl ring **3** was calculated by its highly distorted form accounting for dihedral angle of 7.82, whereas two other phenyl rings **1**-**2** retained planarity as calculated for 1.75 and 1.62.

It can be emphasized that the enhanced planarity directly contributed the improved thermal stability, as summarized in Table 4. In comparisons of the weight reductions for dyes **1**-**6**, it was apparently found that the increased planarity of dye directly contributed to the higher thermal stability, where dye **3** and dye **6** exhibited better stabilities in weight reduction.

The geometry-optimized structures of the fluorescent dyes **1**-**6** were illustrated in Figure 2, and the results of the calculated dihedral angles for dyes **1**-**6** were also summarized in Table 3.

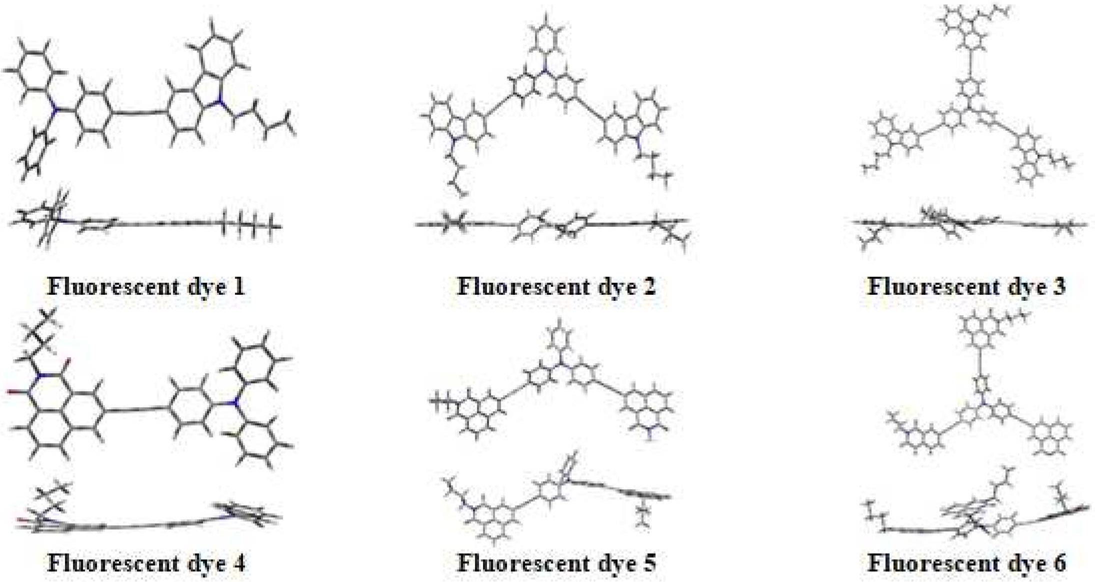

Fig. 2. **Geometry-optimized structures of the fluorescent dyes** 1-6**.**

Table 3

Theoretically calculated dihedral angles.

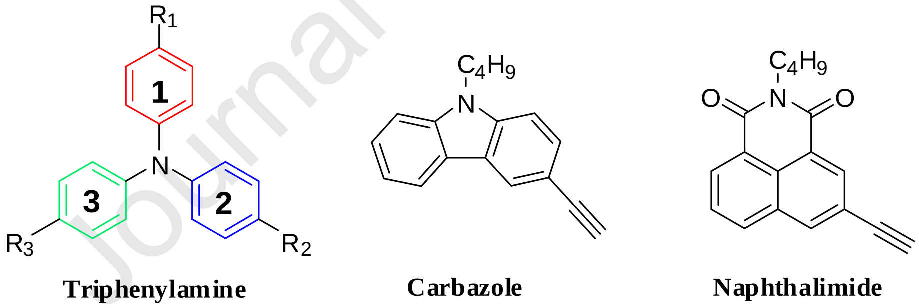

Fluorescent dyes	R_1	R_2	R_3	A (°)			B (°)			Γ (°)		
				1	2	3	1	2	3	1	2	3
1	C	H	H	0.14	3.13	3.19	0.45	-	-	0.32	-	-
2	C	C	H	2.13	2.62	4.68	1.1	1.6	-	1.2	1.4	-
3	C	C	C	0.48	0.39	0.42	0.86	0.79	0.81	0.62	0.54	0.66
4	N	H	H	1.02	3.22	4.02	0.71	-	-	0.60	-	-
5	N	N	H	1.75	1.62	7.82	1.74	1.61	-	0.84	1.02	-
6	N	N	N	0.97	1.13	1.31	6.93	5.30	4.25	6.93	4.17	3.26

*α1(°)=N of triphenylaminebenzene(1) of triphenylamine bond dihedral angles, R1-acetylene bond dihedral angles, α2(°)=N of triphenylamine-benzene(2) of triphenylamine bond dihedral angles, α3(°)=N of triphenylamine-benzene(2) of triphenylamine bond dihedral angles, β1(°)=R1- acetylene bond dihedral angles, β2(°)=R2- acetylene bond dihedral angles, β3(°)=R3- acetylene bond dihedral angles, γ(°)=C- acetylene bond dihedral angles

3.4 Thermal stability of dyes **1-10**

Factors such as π–π interactions, intermolecular hydrogen bonding, and van der Waals forces affect heat resistance; however, in the case of π–π interactions, it becomes sufficiently strong to have a planar molecular structure. The temperature at which the acetylene linkage in the synthesized fluorescent dyes **1–3** was decomposed and the thermal decomposition temperature of the fluorescent dyes was in the range of 297 °C to 333 °C. In case of fluorescent dyes **1** and **2**, the thermal decomposition temperature was 297 °C, which was less than that of fluorescent dye **3**, comprising a structure in which carbazole is twisted around tripheylamine: π–π interaction decreased and the relative paralysis was low. Fluorescent dyes **1** and **2** in which the carbazole moiety was not on the same plane as tripheylamine were thermally decomposed at a temperature less than that of fluorescent dye **3**.

The temperature at which the acetylene linkage of the synthesized fluorescent dyes **4** to **6** was destroyed and the thermal decomposition temperature of fluorescent dyes was in the range of 320 °C to 357 °C. For fluorescent dyes **4** and **5**, the thermal decomposition temperature was 320 °C, which was less than that of fluorescent dye **6**, comprising a structure in which naphthalimide was twisted around triphenylamine, and π–π interactions decreased, with a relatively low heat decomposition temperature. The naphthalimide moiety was not present on the same plane as triphenylamine. Fluorescent dyes **4** and **5** were paralyzed at a temperature less than that of fluorescent dye **6**. When triphenylamine and the substituent were not present in the same plane and became a twisted structure, heat resistance was not satisfactory. For a comparison of the substituent effects between *N*-*n*-butyl group and *N*-phenyl group, it was observed that *N*-phenyl group afforded higher resistance to the weight reductions at 300 °C than that of *N*-*n*-butyl analogue, as shown in table 4. This contribution can be explained by the extended conjugations of π-orbitals, caused by a phenyl ring, resulting in the more efficient delocalization of π-electrons throughout the dye molecule. Therefore, it can also assume that the most substituted analogue **10** by *N*-phenyl carbazole systems in these series exerted the least weight reduction of 0.19 % at 300 °C.

As previously discussed in the calculations of dye structure geometry, the planarity of dye molecule was one of important parameters to affect thermal stabilities. In the series of carbazole substituted dyes **1**-**3**, the less weight reductions observed by the more presence of carbazole substituents those afforded comparatively more planar geometry. The same tendency was found in the corresponding series of dyes **4**-**6**, in which more substitutions by naphthalimide ring and acetylene linkage exerted improved thermal stabilities.

Table 4 summarizes the results of thermogravimetric analysis (TGA) for the dyes **1–10** [31].

Table 4

Thermogravimetric analysis (TGA) of fluorescent dyes **1**–**6**.

Fluorescent Dyes	Thermal stability
	Weight reduction (%, 300 °C)
1	4.40
2	0.76
3	0.23
4	3.20
5	1.81
6	1.93
7	4.20
8	1.02
9	1.65
10	0.19

3.5. TD-DFT and frontier molecular orbital (FMO)

As illustrated in Figure 3, the comparison of the HOMO and LUMO levels of the synthesized fluorescent dyes revealed that the LUMO-level electrons are localized on the substituent carbazole, 1,8-naphthalimide position, while the HOMO level is localized on the triphenylamine position. Hence, electrons are confirmed to be localized by the removal of the alkyl chain and *N*-position substituent in the *N*-position at the LUMO level, verifying that electrons are localized, while the alkyl chain substituents in the *N*-position are structurally twisted. The figure possibly confirmed, but in the case of a fluorescent dyes in which the alkyl chain is substituted at the *N*-position and the acetylene linkage was substituted for the carbazole or 1,8-naphthalimidyl ring, the acetylene linkage in the center the π electrons became delocalized.

The HOMO and LUMO values calculated by the TD-DFT theory revealed similar values for the HOMO (0.07) and LUMO (0.05) for the number of acetylene linkages which due to the interruption in the π-conjugation, including acetylene linkage, by an alkyl chain due to the twisting of the structure; hence, the substituted butyl group does not considerably affect the *N*-position [32-33].

The ΔE values were clearly determined by the effect of the HOMO and LUMO values according to the number of substituents in the acetylene linkage, as shown in Table 5. This trend was observed for all six synthesized fluorescent dyes. By considering the ΔE for each fluorescent dye, the ΔE value for the synthesized fluorescent dyes **1**–**3** exhibited a large difference of 0.09 due to the increase in the π-conjugation when a dye comprising an acetylene linkage exhibits a twisted structure centered on the acetylene linkage.

`

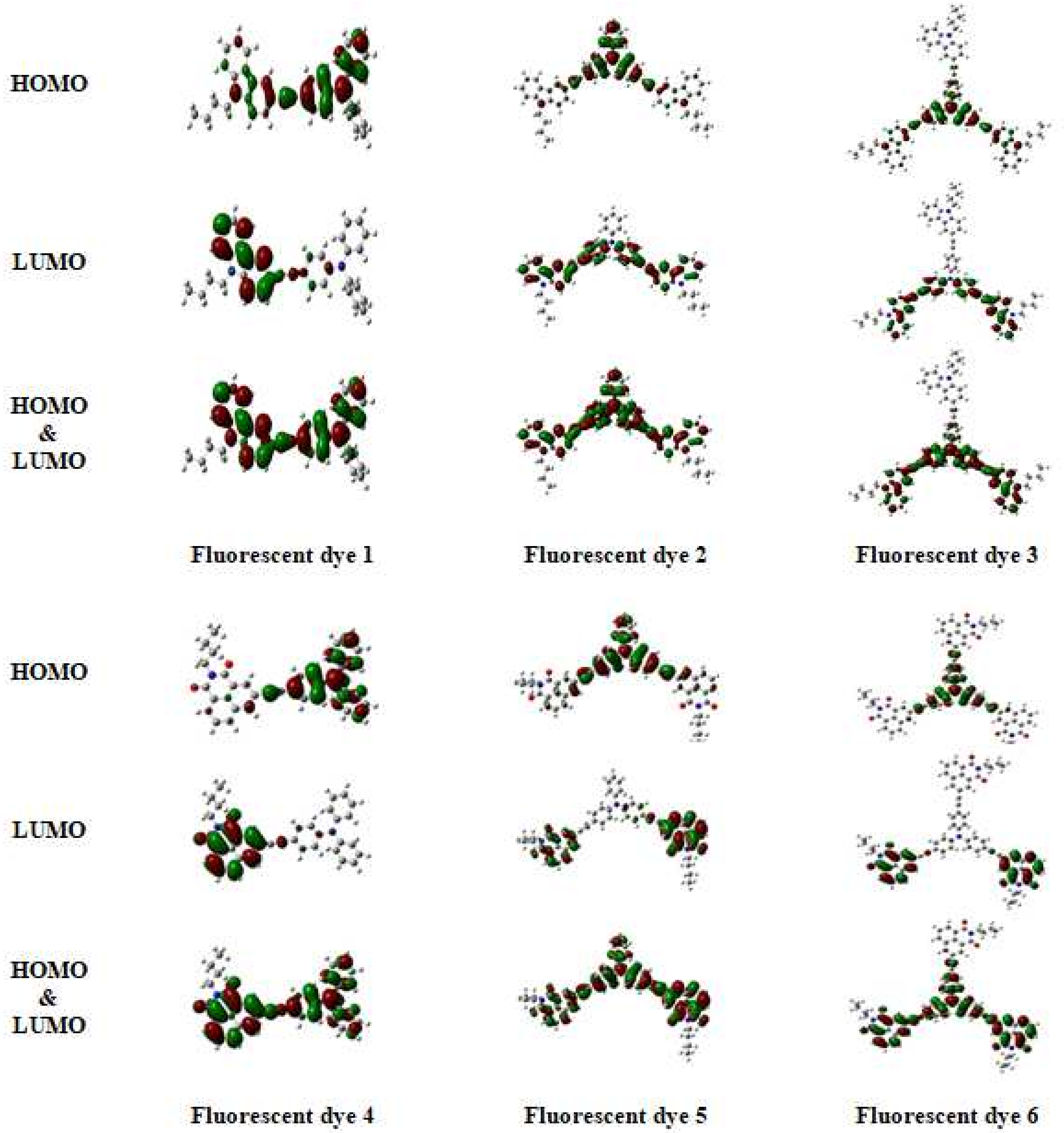

Fig. 3. Molecular orbital models of the HOMOs and LUMOs of fluorescent dyes **1–6**.

The ΔE values were clearly determined by the energy difference between the HOMO and LUMO values according to the number of substituents in the acetylene linkage, as summarized in Table 5. As it was calculated by TD-DFT method, the less ΔE values for dyes **4-6** compared to that of corresponding dyes **1**-**3** can be explained by more efficient π-conjugations arisen from a planar structure between naphthalimide ring and acetylene group [34-35]. In contrast, comparatively less planar forms between carbazole ring and acetylene group can be responsible for the increased ΔE values. These calculated results were in accordance with the observed absorption maxima for dyes **1-6**, as summarized in Table 2.

Table 5
Results of TD-DFT calculations for energy difference values between the HOMO and the LUMO of the synthesized dyes **1-6**.

Fluorescent dyes	HOMO	LUMO	$\Delta E_{\text{(HOMO-LUMO)}}$
1	–7.67	–5.09	2.58
2	–7.62	–5.12	2.50
3	–7.60	–5.14	2.46
4	–7.70	–5.94	1.76
5	–7.78	–6.10	1.68
6	–7.61	–5.96	1.65

3.6. Electron density

From the calculated electron densities for the dyes **1**–**3**, the carbazole system exhibited higher electron densities than the central moiety of triphenylamine that indicated both nitrogen atoms in the carbazole and triphenylamine rings exerted as an electron donor, thus these dyes **1-3** can be a donor-π-donor chromogen. In contrast, other dyes **4**–**6**, higher electron densities of carbonyl groups in the naphthalimidyl ring were calculated, therefore it can be assumed that these carbonyl groups may act as an electron acceptor leading to stronger donor-π-acceptor chromogen [36-37]. The calculated electron densities of dyes **1-6** were illustrated in Figure 4.

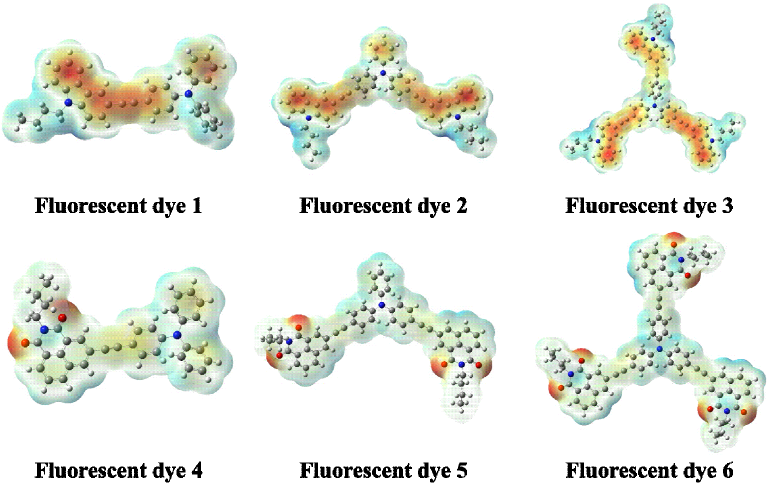

Fig. 4. Electron densities of fluorescent dyes **1**–**6**.

4. Conclusions

Judging from the absorption maxima of dyes **1-6** prepared, it was found that increase of the number of acetylene group which introduced to the triphenylamine moiety readily exhibited a bathochromic shift. This red shifts can be attributable to the increased conjugation of π-orbitals. It was unusual that the absorption maxima of dyes **4-6** substituted by naphthalimidyl group were bathochromic shifted significantly comparing to the corresponding dyes **1-3** which containing the same number of carbazole analogous. These red shifts may be arisen by the more efficient conjugations between central triphenylamine system and naphthalimidyl group via an acetylene linkage group than performed by corresponding carbazole analogous due to the retention of planarity of π-conjugations throughout the dye molecule for naphthalimidyl based dyes **4-6**. It was also observed that the presence of a *N*-phenyl ring in the carbazole system created a bathochromic shift comparing to that of *N*-*n*-butyl group that can be also attributable to the increased π-conjugations.

Both contributions of the bathochromic shifts at absorption maxima and larger Stokes' shifts by naphthalimidyl substituted dyes **4-6** readily provide a red emission, whereas the corresponding carbazole substituted dyes emitted a blue fluorescence. In contrast, two dyes **9-10** containing a central moiety of triphenyltriazine exhibited comparatively larger Stokes' shifts than that of corresponding triphenylamine based analogous **1-3** combined with a bathochromic shift in absorption maxima leading to a green fluorescence emission.

From the geometry analysis based on the TD-DFT theory of the six synthesized fluorescent dyes, carbazole-based fluorescent dyes **1–3** did not exhibit the twisting of the substituents at the *N*-position, and naphthalimide-based fluorescent dyes **4–6** exhibit a planar structure with the 1,8-naphthalimide and carbazole moieties located in the same plane except for the twisting of the substituents at the *N*-position.

In terms of quantum yield, there was a tendency that dyes **7–10** containing a central moiety of triphenyltriazine or diphenylsulfone exhibited consistently higher quantum yields of 0.83 to 0.85, whereas the other dyes **1–6** varied their quantum yields from 0.34 to 0.89 depending on the substituent.

With respect to heat stability, carbazole- and naphthalimide- based fluorescent dyess exhibited thermal decomposition temperatures of >250 °C and >300 °C, respectively. The introduction of acetylene linkages in fluorescent dyes improved the planarity, which in turn lead to excellent heat resistance due to the considerably strong π–π interactions.

Acknowledgements

This work was supported by the Technology Innovation Program funded by the Ministry of Trade, Industry and Energy (KOREA).

References

[1] Kim T.H., Kwon S.H., Choi J.H. Synthesis and properties of blue fluorescent dyes based on diphenylamine by introducing an acetylene linkage group with carbazole and 1,8-naphthalimide. Bulletin of the Korean Chemical Society 2019;40:1229-1232.

[2] Gudeika D., Grazulevicius J.V., Volyniuk D., Juska G., Jankauskas V., Sini G. Effect of ethynyl linkages on the properties of the derivatives of triphenylamine and 1,8-naphthalimide. The Journal of Physical Chemistry 2015;119:28335-28337.

[3] Kato S.I., Noguchi H., Kobayashi A., Yoshihara T., Tobita S., Nakamura Y. Bicarbazoles: Systematic structure-property investigations on a series of conjugated carbazole dimers. The Journal of Organic Chemistry 2012;77:9120-9124.

[4] Kim K.W., Kim G.H., Kwon S.H., Yoon H.I., Son J.E., Choi J.H. Synthesis and photophysical properties of blue-emitting fluorescence dyes derived from naphthalimide derivatives containing a diacetylene linkage group. Dyes and Pigments 2018;158: 353-361.

[5] Xia Q., Batentschuk M., Osvet A., Richter P., Häder D. P., Schneider J., Winnacker A. Enhanced photosynthetic activity in Spinacia oleracea by spectral modification with a photoluminescent light converting material. Optics express 2013;21(106): A909-A916.

[6] Gao Y., Bulusu S., Zeng X. C. Gold-caged metal clusters with large HOMO− LUMO gap and high electron affinity. Journal of the American Chemical Society 2005;127(45):15680-15681.

[7] Huang B., Yin Z., Ban X., Ma Z., Jiang W., Tian W., Sun Y. Nondoped deep blue OLEDs based on Bis-(4-benzenesulfonylphenyl)-9-phenyl-9*H*-carbazoles. Journal of Luminescence 2016;172:7-13.

[8] Senol R., Kilic S., Tasdelen K. Pulse timing control for LED plant growth unit and effects on carnation. Computers and Electronics 2016;123:125-134.

[9] Kogure T., Kawano H., Abe Y., Miyawaki A. Fluorescence imaging using a fluorescent protein with a large Stokes shift. Methods 2008;45(3):223-226.

[10] Elegemeie G.H., Moamed R.A. Microwave synthesis of fluorescent and luminescent dyes(1990-2017). Journal of Molecular Structure 2018;1173:707-742.

[11] Jang H.Y., Namgoog J. W., Sung M. G., Chang Y. K.., Kim J.P. Synthesis and characterization of fluorescent dyes and their applications for the enhancement of growth rate of *Chlorella vulgaris.* Dyes and Pigments 2018;158: 148-149.

[12] Reddy T.S., Hwang J.Y., Mi H., Choi M.S. Aggregation induced emission properties of naphthalimide-coumarin conjugates with various intermolecular linkages. Dyes and Pigments 2018;158:415-416.

[13] Kotowicz S., Korzec M., Siwy M., Golba S., Malecki J.G., Janeczek H., Mackowski S., Bednarczyk K., Libera M., Schab-Balcerzak E. Novel 1,8-naphthalimdes substituted at 3-C position: Synthesis and evaluation of thermal, electrochemical and luminescent properties. Dyes and Pigments 2018;158:68-73.

[14] Li X., Gu J., Huang H., Zhou Z., Gao J., Wang Q. Carbazole based new organic dye recognizes hydrazine and hydrogen sulfide via signal difference protocols. Dyes and Pigments 2020;181:108545.

[15] Bag S.S., Jana S., Sasula M. Sonogashira Cross-Coupling:Alkyne-Modified Nucleosides and Their Applications. Palladium Catalyzed Modification of Nucleosides. Nucleotides and Oligonucleotides 2018;75-146.

[16] Kim S.H., Ryu J.H., Choi H.J., Kim H.S. Electrochromic properties of new fluorophores containing triphenylamine moiety. Dyes and Pigments 2005;64(3):279-281.

[17] Fang Q., Xu B., Jiang B., Fu H., Zhu W., Jiang X., Zhang Z. A novel fluorine derivative containing four triphenylamine groups: Highly thermostable blue emitter with hole transporting ability for organic light emitting diode (OLED). Synthetic Metals 2005;155(1):206-210.

[18] Lei Y., Niu Q., Mi H., Wang Y., Nurulla I., Shi W. Carbazole-based conjugated polymer with tethered acetylene groups: Synthesis and characterization. Dyes and Pigments 2013;96(1):138-147.

[19] Wang J., Chen Y., Li F., Zong X., Guo J., Sun Z., Xue S. A new carbazole-based hole transporting material with low dopant content for perovskite solar cells. Electrochimica Acta 2016;210:673-680.

[20] Wang W.D., Hu Y., Li Q., Hu S.L. A carbazole-based turn on fluorescent probe for the detection of hydrazine in aqueous solution. Inorganica Chimica Acta 2018;477:206-211.

[21] Mestiri T., Chemek M., Rouabeh J., Alimi K. DFT and TD-DFT modeling of new carbazole-based oligomers for optoelectronic devices. Computational Condensed Matter 2015;4:23-31.

[22] Ramalingam S., Karabacak M., Periandy S., Puviarasan N., Tanuja D. Spectroscopic (infrared, Raman, UV and NMR) analysis, Gaussian hybrid computational investigation (MEP maps/HOMO and LUMO) on cyclohexanone.

[23] Hagberg D.P., Marinado T., Karlsson K.M., Nonomura K., Qin P., Boschloo G. Tuning the HOMO and LUMO energy levels of organic chromophores for dye sensitized solar cells. The Journal of organic chemistry 2000;72(25):9550-9556.

[24] Zade S.S., Bendikov M. From oligomers to polymer: convergence in the HOMO−LUMO gaps of conjugated oligomers. Organic letters 2006;8(23):5243-5246.

[25] Lee H.Y., Kim K.W., Park C.E., Kim G.H., Choi J.H. Novel Ethyne-linked compounds containing 1, 8-naphthalimide group for light conversion film. In MATEC Web of Conferences 2016;67: 10-16.

[26] Kim K.W., Kim G.H., Park C.E., Choi J.H. 1,8-Naphthalimide derivatives containing ethynyl linkage and blue light emitting properties. Bulletin of the Korean Chemical Society 2017;38:956-959.

[27] De Silva A.P., Gunaratne H.N., Gunnlaugsson T., Huxley A.J., McCoy C.P., Rademacher J.T., Rice T.E. Signaling recognition events with fluorescent sensors and switches. Chemical reviews 1997;97(5): 1515-1566.

[28] Park H.J., Yu S.J., Anil K., Yi Y.G., Kim J.H., Han T.S. Fabrication of Current Intensity Convertible CLD of Large Current Intensity for LED Network Application. Journal of the Korean Institute of Electrical and Electronic Material Engineers 2012;25(9): 723-726.

[29] Sheridan M.V., Lam K., Geiger W.E. An anodic method for covalent attachment of molecules to electrodes through an ethynyl linkage. Journal of the American Chemical Society 2013;135(8):2939-2942.

[30] Sheridan M.V., Lam K., Geiger W.E. An anodic method for covalent attachment of molecules to electrodes through an ethynyl linkage. Journal of the American Chemical Society 2013;135(8):2939-2942.

[31] Pedmale U.V., Huang S.C., Zander M., Cole B.J., Hetzel J., Ljung K., Chory J. Cryptochromes Interact Directly with PIFs to control plant growth in limiting blue light. Cell 2016;164(1-2):233-245.

[32] Tigreros A., Ortiz A., Insuasty B. Effect of π-Conjugated linkage on photophysical properties: Acetylene linker as the better connection group for highly solvatochromic probes. Dyes and Pigments 2014;111:45-51.

[33] Kim D., Cho H., Kim C. Blue light emitting polymers. Progress in Polymer Science 2000;25(8):1089-1139.

[34] Belieres M., Sartor V., Fabre P.L., Poteau R., Bordeau G. Chouinilalanne, N. Simple electron donor molecules based on triphenylamine and carbazole derivatives. Dyes and Pigments 2018;153:275-283.

[35] Schlegel H.B. Optimization of equilibrium geometries and transition structures. Journal of Computational Chemistry 1982;3(2):214-218.

[36] Li X., Frisch M.J. Energy-represented direct inversion in the iterative subspace within a hybrid geometry optimization method. Journal of chemical theory and computation 2006;2(3):835-839.

[37] Cekaviciute M., Simokaitiene J., Sych G., Grazulevicius J.V., Jankauskas V., Volyniuk D., Ivanyuk K. Diphenylethyenyl and methylphenylethynyl-substituted triphenylamines as effective hole transporting and emitting materials. Dyes and Pigments 2016;134:593-600.

- Tables -

Table 1

Calculated absorption maxima and F values for fluorescent dyes **1–6**.

Fluorescent dyes	Calculated absorption maxima (nm) and F values	
	λ_{max}^{cal}	F
1	330	1.57
2	333	1.39
3	357	1.42
4	418	1.61
5	430	1.57
6	431	1.98

Table 2

Absorption and fluorescence properties of the synthesized dyes.

Fluorescent dyes	λ_{max}^{ab} (nm)	λ_{max}^{em} (nm)	Stokes shift (nm)	ε_{max} ($dm^3\ mol^{-1}\ cm^{-1}$)	Quantum yield
1	330	401	71	16,000	0.68
2	336	416	80	17,000	0.72
3	341	430	89	16,000	0.89
4	432	580	148	17,000	0.34
5	436	595	159	18,000	0.44
6	440	604	164	19,000	0.78
7	346	444	98	43,000	0.83
8	358	452	94	44,000	0.85
9	362	502	140	41,000	0.83
10	370	515	145	42,000	0.85

λ_{max}^{ab}, λ_{max}^{em}: determined in methylene chloride(1.0×10^{-5} mol/L)

Reference: Anthracene.

Table 3

Theoretically calculated dihedral angles.

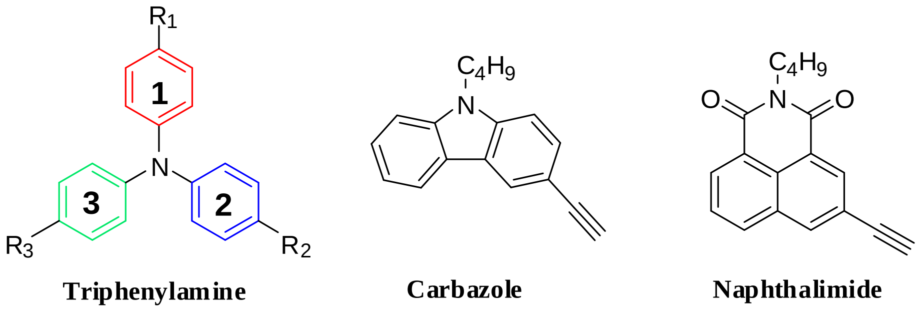

Fluorescent dyes	R_1	R_2	R_3	A (°)			B (°)			Γ (°)		
				1	2	3	1	2	3	1	2	3
1	C	H	H	0.14	3.13	3.19	0.45	-	-	0.32	-	-
2	C	C	H	2.13	2.62	4.68	1.1	1.6	-	1.2	1.4	-
3	C	C	C	0.48	0.39	0.42	0.86	0.79	0.81	0.62	0.54	0.66
4	N	H	H	1.02	3.22	4.02	0.71	-	-	0.60	-	-
5	N	N	H	1.75	1.62	7.82	1.74	1.61	-	0.84	1.02	-
6	N	N	N	0.97	1.13	1.31	6.93	5.30	4.25	6.93	4.17	3.26

*α1(°)=N of triphenylaminebenzene(1) of triphenylamine bond dihedral angles, R1-acetylene bond dihedral angles, α2(°)=N of triphenylamine-benzene(2) of triphenylamine bond dihedral angles, α3(°)=N of triphenylamine-benzene(2) of triphenylamine bond dihedral angles, β1(°)=R1- acetylene bond dihedral angles, β2(°)=R2- acetylene bond dihedral angles, β3(°)=R3- acetylene bond dihedral angles, γ(°)=C- acetylene bond dihedral angles

Table 4

Thermogravimetric analysis (TGA) of fluorescent dyes **1**–**6**.

Fluorescent Dyes	Thermal stability
	Weight reduction (%, 300 °C)
1	4.40
2	0.76
3	0.23
4	3.20
5	1.81
6	1.93
7	4.20
8	1.02
9	1.65
10	0.19

Table 5

TD-DFT results for excitation from the HOMO to the LUMO of the synthesized dyes.

Fluorescent dyes	HOMO	LUMO	$\Delta E_{\text{(HOMO-LUMO)}}$
1	–7.67	–5.09	2.58
2	–7.62	–5.12	2.50
3	–7.60	–5.14	2.46
4	–7.70	–5.94	1.76
5	–7.78	–6.10	1.68
6	–7.61	–5.96	1.65

- Figures & Schemes -

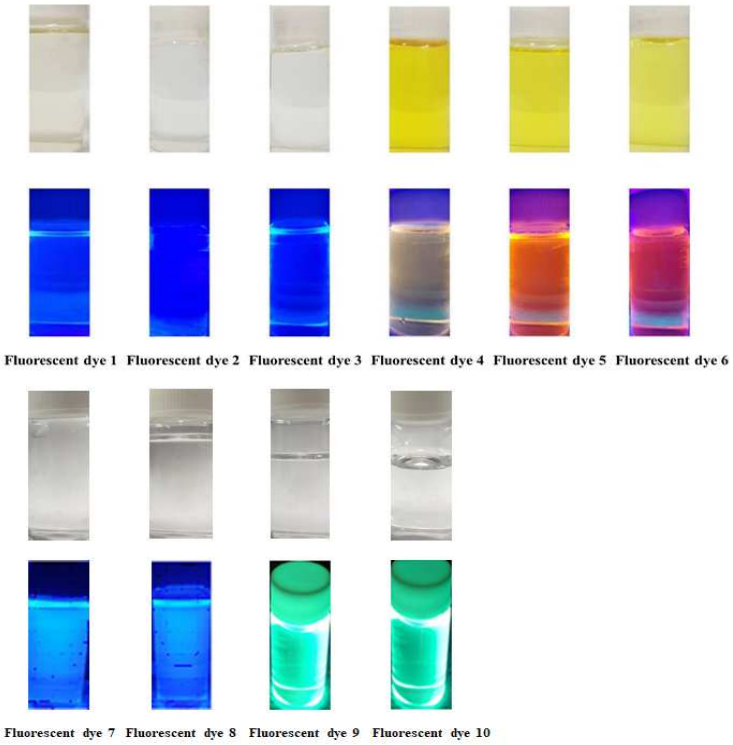

Fig. 1. Optical images of fluorescent dyes **1–10** in methylene chloride solutions (100 ppm) under a UV light of 365 nm.

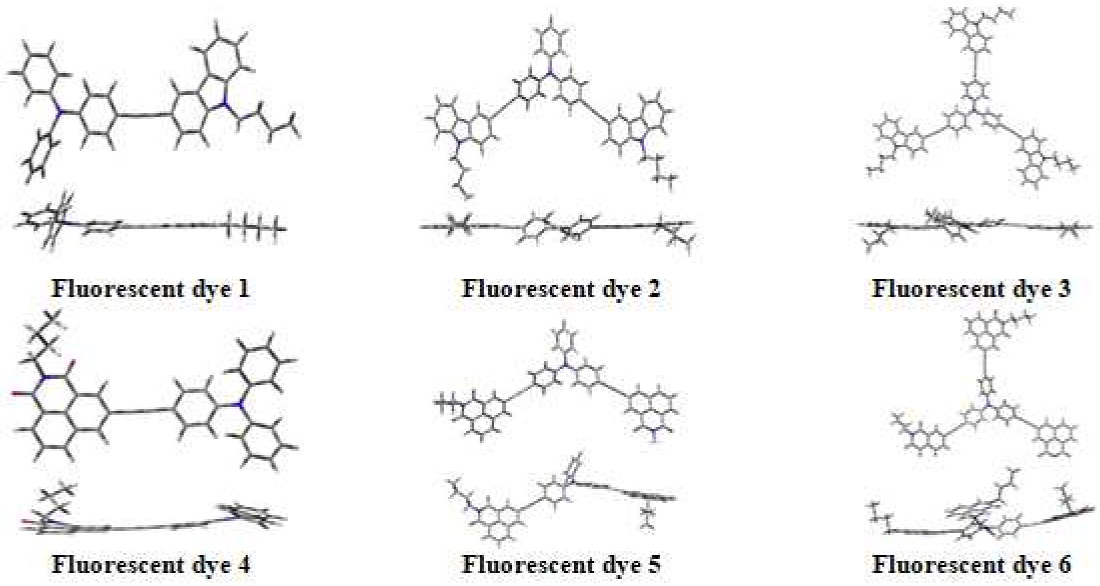

Fig. 2. Geometry-optimized structures of the fluorescent dyes **1-6**.

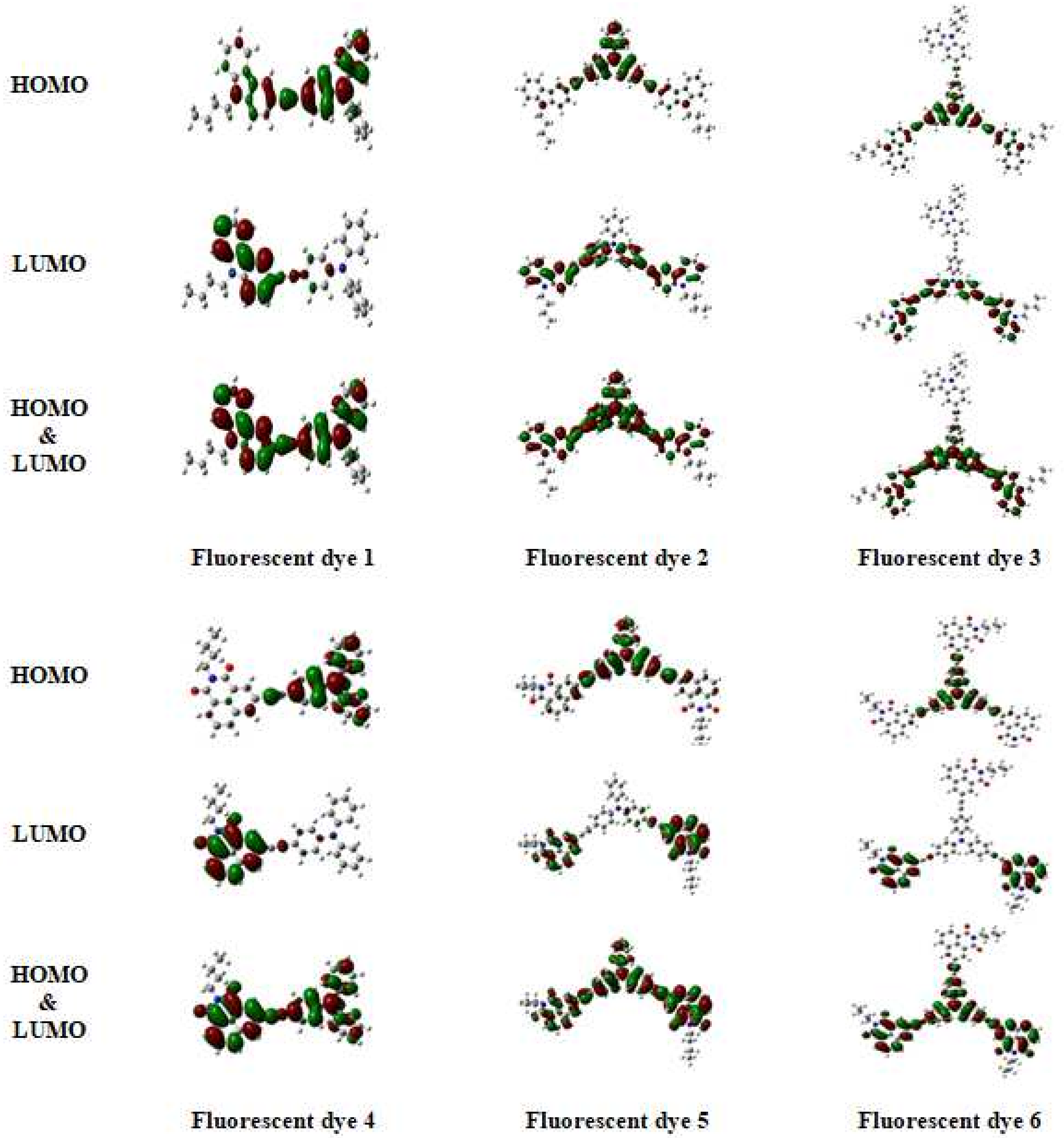

Fig. 3. Molecular orbital models of the HOMOs and LUMOs of fluorescent dyes **1–6**.

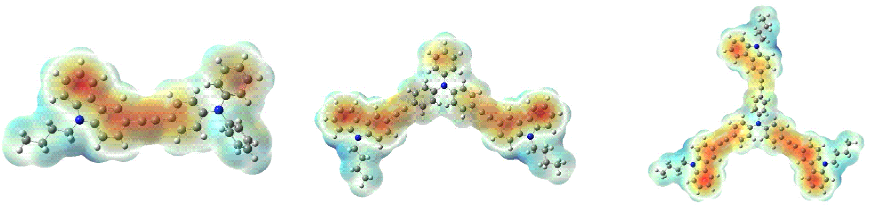

Fluorescent dye 1 **Fluorescent dye 2** **Fluorescent dye 3**

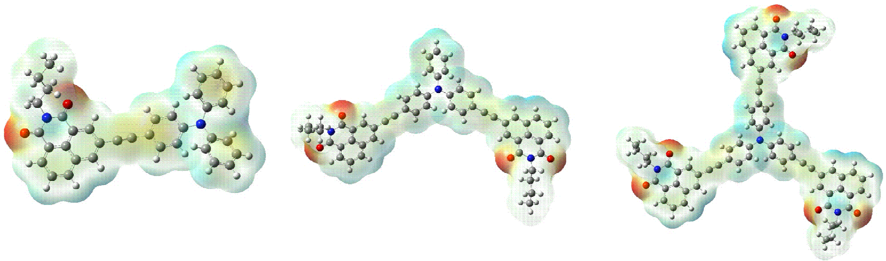

Fluorescent dye 4 **Fluorescent dye 5** **Fluorescent dye 6**

Fig. 4. Electron densities of fluorescent dyes **1–6**.

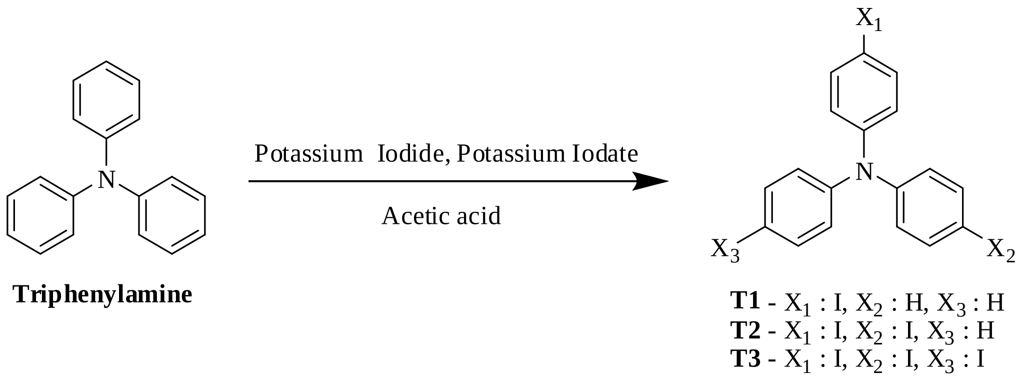

Scheme 1. Synthesis of the triphenylamine derived dye intermediates **T1**-**T3**.

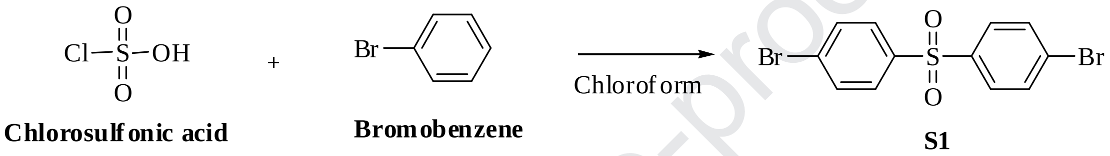

Scheme 2. Synthesis of the diphenyl sulfone derived dye intermediates **S1**.

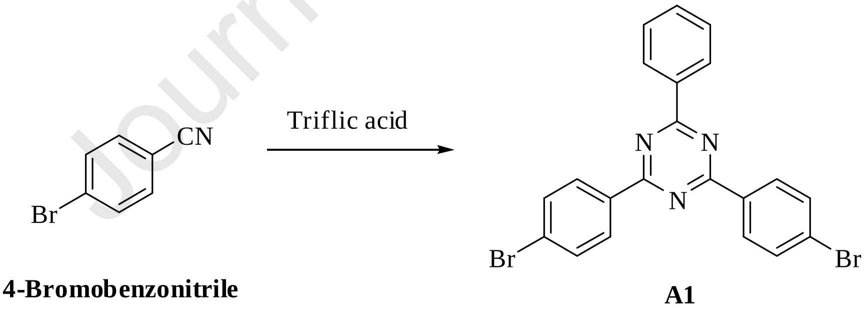

Scheme 3. Synthesis of the triazine derived dye intermediates **A1**.

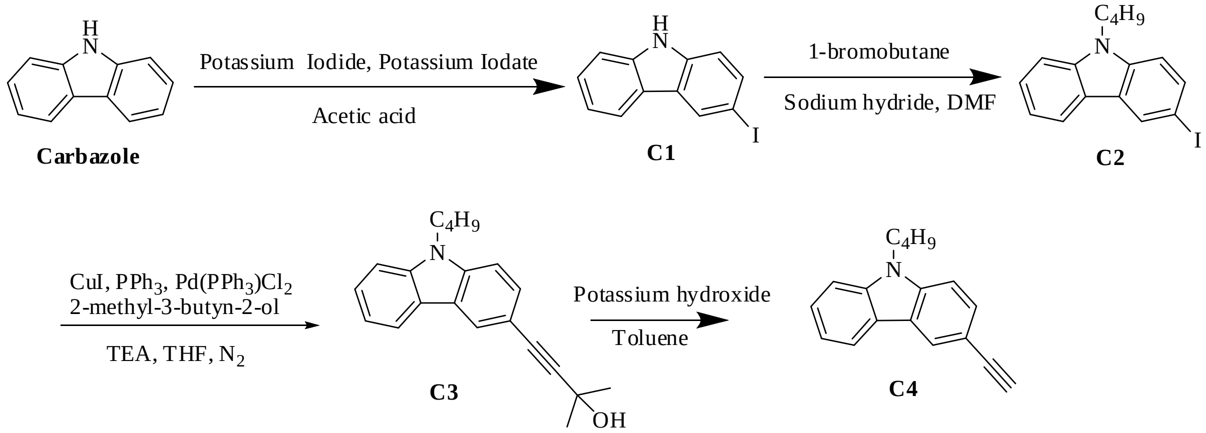

Scheme 4. Synthesis of the carbazole derived dye intermediates **C1**-**C4** [1].

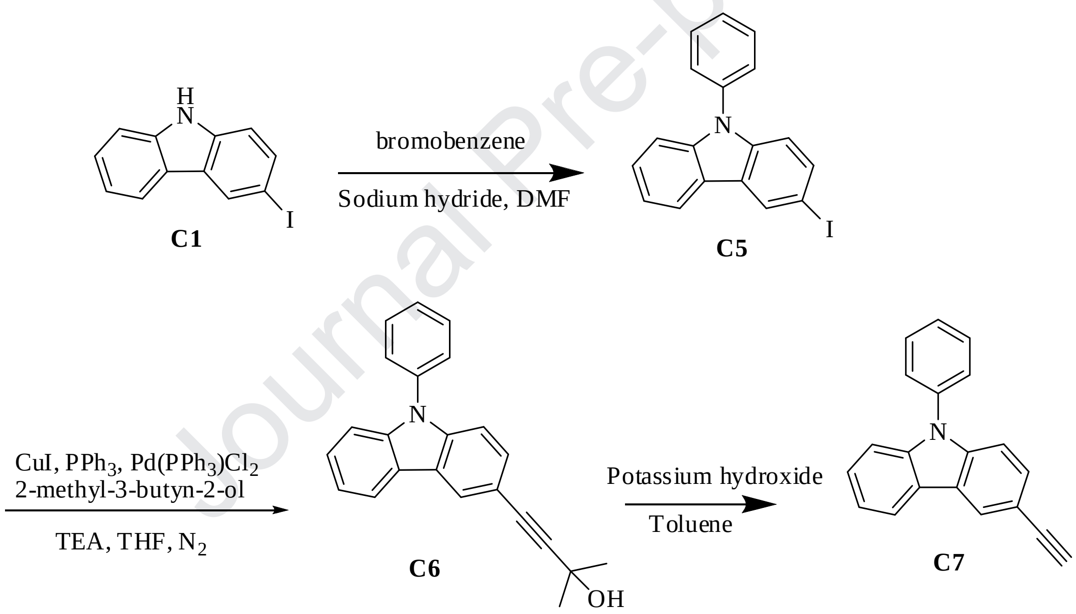

Scheme 5. Synthesis of the carbazole derived dye intermediates **C5-C7**.

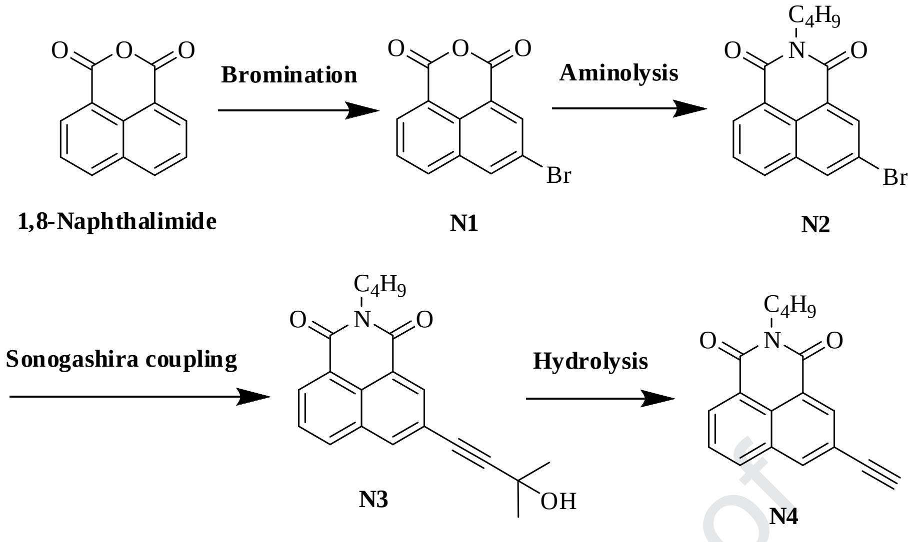

Scheme 6. Synthesis of the naphthalimidyl dye intermediates **N1**-**N4**.

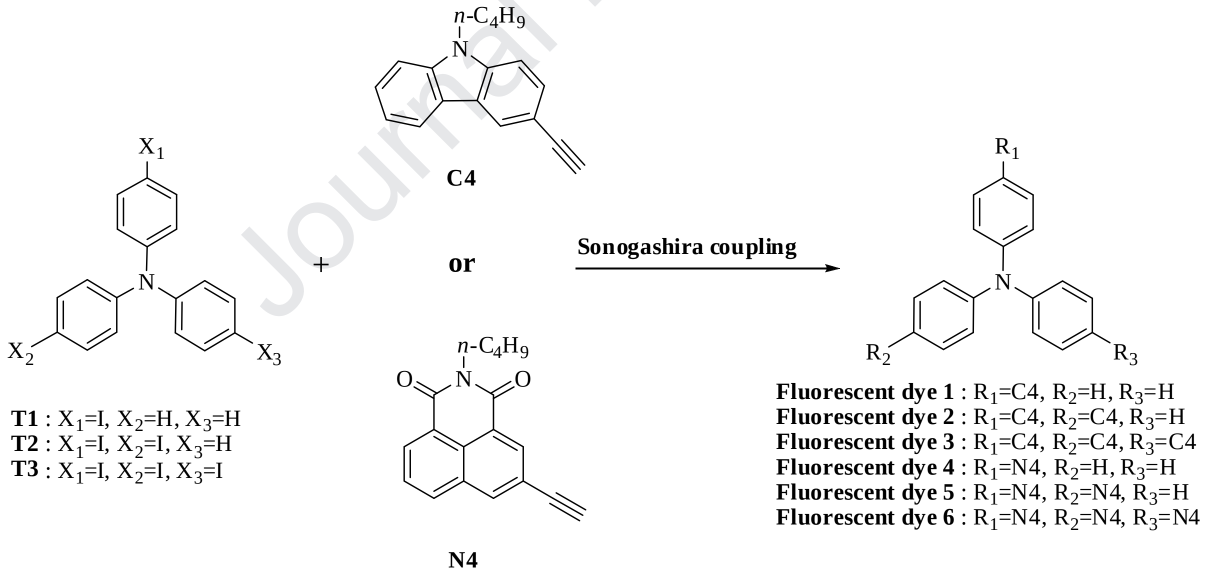

T1 : X_1=I, X_2=H, X_3=H
T2 : X_1=I, X_2=I, X_3=H
T3 : X_1=I, X_2=I, X_3=I

Fluorescent dye 1 : R_1=C4, R_2=H, R_3=H
Fluorescent dye 2 : R_1=C4, R_2=C4, R_3=H
Fluorescent dye 3 : R_1=C4, R_2=C4, R_3=C4
Fluorescent dye 4 : R_1=N4, R_2=H, R_3=H
Fluorescent dye 5 : R_1=N4, R_2=N4, R_3=H
Fluorescent dye 6 : R_1=N4, R_2=N4, R_3=N4

Scheme 7. Synthetic routes of fluorescent dyes **1–6**.

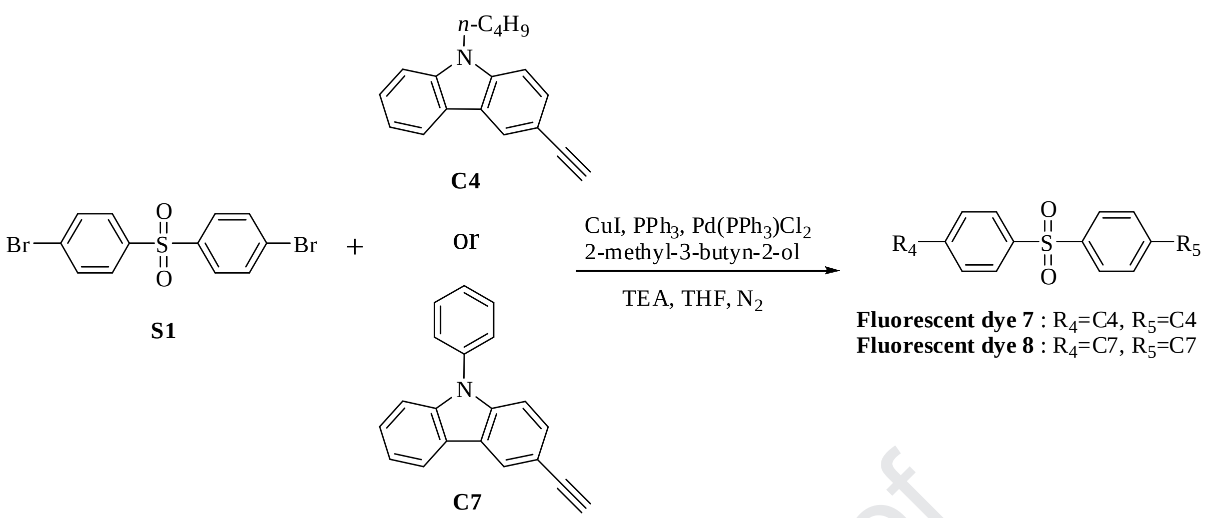

Scheme 8. Synthetic routes of fluorescent dyes **7–8**.

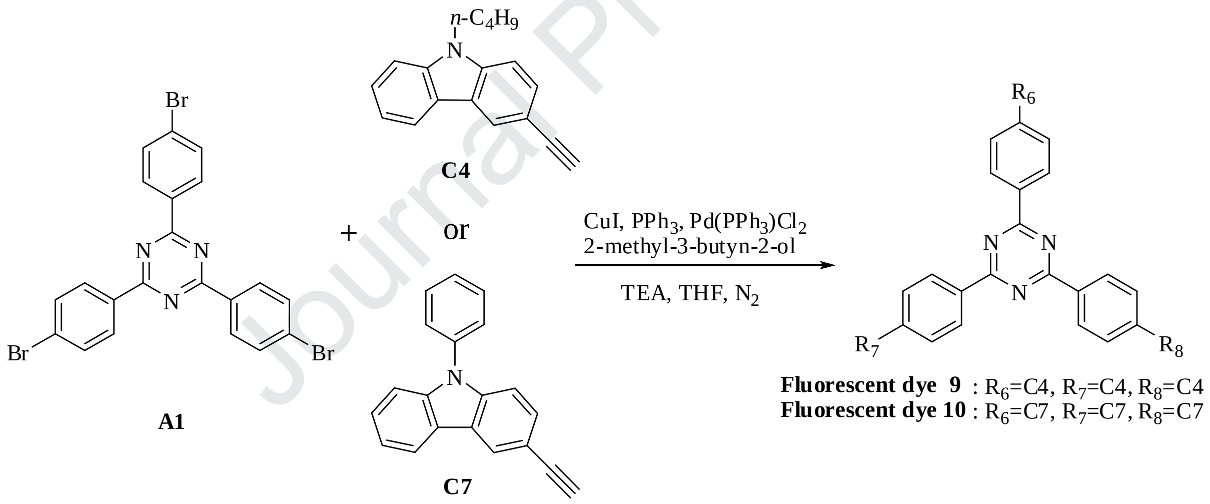

Scheme 9. Synthetic routes of fluorescent dyes **9–10.**

Highlights

- Fluorescence dyes to provide three different ranges of emission, blue, green, and red fluorescence.
- Dyes containing an acetylene linkage group between *N*-butyl carbazole or corresponding naphthalimidyl moiety and triphenylamine central group.
- Dyes containing an acetylene linkage group between *N*-butyl carbazole or *N*-phenyl carbazole and diphenyl sulfonyl central group.
- Dyes containing an acetylene linkage group between *N*-butyl carbazole or *N*-phenyl carbazole and triphenyl triazine central group.
- Improved thermal stabilities by the increased numbers of substitution.

Author statement

Jae-Hong Choi : Supervision, Writing, Submission, Revision

Kyung-Won Kim : Dye synthesis, Analysis of dye structure, Calculations of TD-DFT, Writing original-draft

Su-Hyeon Kwon : Dye synthesis, Analysis of dye structure

Byung-Jun Lee : Dye synthesis, Analysis of dye structure

Sung-Ok Ahn : Dye synthesis, Analysis of thermal-stabilities, Analysis of absorption & fluorescence properties

Ju-Hong Lee : Dye synthesis, Analysis of dye structure, Revision of draft

Declaration of interests

☒ The authors declare that they have no known competing financial interests or personal relationships that could have appeared to influence the work reported in this paper.

☐The authors declare the following financial interests/personal relationships which may be considered as potential competing interests:

The authors declare that they have no known competing financial interests or personal relationships that could have appeared to influence the work reported in this paper.